

Deep Learning based 5G mm-Wave Beamforming management scheme

Rigobert TSOUAPI

African Institute for Mathematical Sciences (AIMS), Senegal

Supervised by: Ado Adamou ABBA ARI, Ph.D., MBA

LI-PaRAD Lab, University of Versailles Saint-Quentin-en-Yvelines, France

LaRI Lab, University of Maroua, Cameroon

September 8, 2021



AIMS

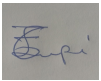
African Institute for
Mathematical Sciences
SENEGAL

DECLARATION

This work was carried out at AIMS Senegal in partial fulfilment of the requirements for a Master of Science Degree.

I hereby declare that except where due acknowledgement is made, this work has never been presented wholly or in part for the award of a degree at AIMS Senegal or any other University.

Student: Rigobert TSOUAPI



ACKNOWLEDGEMENTS

I am specially grateful to **Professor Neil Geoffrey Turok** founder of African Institute for Mathematical Sciences (AIMS) for making a reality his great initiative where I learnt a lot.

I would like to express my gratitude to **Dr. Ado Adamou ABBA ARI** who proposed this interesting topic at the cutting edge of mobile technology, and have accept to helped and supported me through work with the thesis. He have guided me through the whole process, he always provided me with all the documents I needed to better understand the subject. Reading my first draft and patiently waited for my last.

I sincerely thank **Dr. Amy SADIO** who was my principal tutor, for her carefully reading and help for better explanation of sentences, sometime asked uncomfortable question that help me to better developed my idea.

I thank **Noutegne Tcheup Lionel SEDAR** for contributing new ideas and answering some of my questions about optimization and modelling.

I am appreciative of both academic non academic staff of AIMS for creating home environment of work.

I thank all my AIMS colleagues and all who worked or wrote their thesis here at AIMS for their friendliness and great atmosphere. Really the best place to write a thesis.

Last, My parents, sister and friends for helping me think of something else than SNR, beamforming, Deep learning and references sometimes.

DEDICATION

I dedicate this thesis to my family.

Abstract

In 5G New Radio environment, mm-Wave is the key technology that enables the higher data rate. Because of the high path-loss at mm-Wave frequencies and high throughput demands of 5G New Radio systems, it is crucial to the user to always stay connected to the most suitable station and beam. Therefore beam management and interference coordination become crucial to obtain the fine alignment of each single beam. Beam management operation brings optimization problem that can be easily solved today by Machine Learning model especially Deep Learning. In this thesis we built an optimization problem in context of Dense mm-Wave and propose the approach solution using block coordinate descent method. We built the Deep Neural Network model with 3 hidden layers that can take the data generated in the optimization problem step. The results show that the computational time is more less with deep neural networks (DNN) approach for the same result compared to the classical approach of beam management.

Key words: 5G, mm-Wave, beamforming, Deep Learning, Deep Neural Network.

Contents

Declaration	i
Acknowledgements	ii
Dedication	iii
Abstract	iv
Introduction	1
Background of the study	1
Problem statement	1
Research Objective	2
Organisation of the work	2
1 Overview of key concepts in 5G mobile network	3
Introduction	3
1.1 Millimeter-Waves	3
1.1.1 Definition of millimeter waves	3
1.1.2 Characteristics of mm-Waves	3
1.1.3 Capacity Bandwidth in free and non free-space transmission power	4
1.1.4 Operating Bandwidth for Wireless communication	4
1.2 Massive MIMO system	4
1.2.1 MIMO system	5
1.2.2 Massive Multi-users MIMO	5
1.2.3 Potentials and characteristics of massive MIMO	6
1.2.4 Limitation of massive MIMO	7
1.3 Antenna selection	7
1.3.1 System Model	8
1.3.2 Optimal antenna subset selection	9
1.4 Beam management and interference coordination	9

1.4.1	Beamforming	10
1.4.2	Beam management	10
1.4.3	Interference coordination	12
	Conclusion	14
2	Survey of existing Machine Learning based scheme for beam management and interference coordination	15
	Introduction	15
2.1	Machine Learning presentation	15
2.1.1	General schema for machine learning methods	15
2.1.2	Machine learning techniques and algorithms	16
2.2	Deep Learning	17
2.2.1	Neural Networks	17
2.2.2	Deep Learning activation function	18
2.2.3	Deep Learning algorithms	19
2.3	Insighth of Deep Learning based Beam management and interference coordination	21
	Conclusion	22
3	5G mm-Wave systems modeling and beamforming mechanism based on Deep Learning	23
	Introduction	23
3.1	System model for mm-Wave massive MIMO system	23
3.1.1	Efficient Beamforming training mechanism for dense mm-Wave network	24
3.2	Problem formulation	26
3.3	Beam management and interference coordination in Dense mm-Wave network .	29
3.3.1	Beamforming Training Information Aided Beam Management and Inter- ference Coordination	29
3.3.2	The proposed approach solution of problem P2	30
3.4	Deep Learning based Beam Management and Interference Coordination	32
3.4.1	System Setup	32
3.4.2	DNN structure	33
3.4.3	Data Generation	34

3.4.4	Training stage	34
3.4.5	Testing stage	35
	Conclusion	35
4	Numerical Simulation and Performance evaluation	36
4.1	The performance of efficient Beamforming Training Mechanism	36
4.1.1	Evaluation of the impact of the number of <i>AP</i> and <i>STA</i>	36
4.1.2	Evaluation of the impact of the beamwidth	37
4.2	The performance of Deep Learning Based Beam Management	38
4.2.1	Simulation setup	38
4.2.2	Parameters selection and performance of DNN approach	39
4.2.3	Sum-rate performance	40
	Conclusion	41
	Conclusion and perspectives	42
	References	45

List of Figures

1.1	MIMO System.	5
1.2	Transmit antenna selection with MRC Dong et al. (2008)	8
1.3	Illustration of transmit and receive training for downlink beamspace MU-MIMO Xue et al. (2018)	11
1.4	5G interferences management issues Qamar et al. (2019).	12
2.1	Schema for ML methods.	16
2.2	Venn diagram of the relation between deep learning, ML, and AI Zhang et al. (2019).	16
2.4	A CNN architecture Wang et al. (2017).	20
2.5	A RNN architecture Zhang et al. (2019).	20
3.1	Dense mm-Wave network architecture.(Zhou et al., 2018)	23
3.2	BFT mechanism in dense mm-Wave.	24
3.3	System model of DNN based LSAP	32
3.4	DNN structure for j-th sub-assignment problem.	33
4.1	The overhead of IEEE802.11ad/ay BFT.	36
4.2	The overhead of proposed BFT mechanism.	37
4.3	The performance between BFT in IEEE802.11ad/ay and proposed efficient BFT mechanism	38
4.4	SNR values Data Frame	39
4.5	learning rate selection	40
4.6	Sum-rate and computational time performance of DNN and BM-IC when the number of STA increase	41

List of Tables

2.1	Ativation Functions	19
4.1	Simulation parameters	39
4.2	Sum-rate and computational time performance of DNN and BM-IC	40

Introduction

Background of the study

Explosion of the internet and its contents cause the ever growing traffic demand and ultra high speed wireless communication such as microwave bands (eg. sub-6G) which was the main technology using became insufficient compared to the high traffic need due to its limited spectrum. Therefore, the mm-Wave that have rich spectrum resources are able to support high data rate wireless communications, became the key technology of the fifth generation mobile communication systems (5G) [Zhou et al. \(2018\)](#). However, mm-Wave frequencies makes the channel conditions highly vulnerable, the signals face severe pathloss as well as penetration losses, lower diffraction, and high oxygen absorption. Due to the short wave length of the mm-Wave bands, a large number of antennas, massive Multiple-Input-Multiple-Output (massive MIMO) may be deployed on a small size device in order to realize high-quality mm-Wave communications and long-distance using antenna array technology [Sharma et al. \(2017\)](#). This massive MIMO system enhances the Signal-to-Noise Ratio (SNR), especially at the reception side.

In 5G, mm-Wave beamforming is the important and necessary technique to use for achieve the best SNR. The basic idea of beamforming is to concentrate the transmit signal from the antenna in the direction of the intended receiver and therefore significantly improving the received signal power. This is done by altering the phase of the signals from each antenna element in a way that the signals add up constructively in the intended direction and destructively in other directions. To establish and retain a suitable beam for an intended receiver, the beams require fine alignment. This is achieved through a set of operations collectively known as beam management which includes beam establishment, beam refinement and beam tracking (beamforming training mechanism BFT). Achieving perfectly aligned beams, power and beamwidth between transmitter and receiver requires an intelligent algorithm that in an efficient way can select the most suitable beam based on the learning process of such thresholds parameters.

The recent appearance of the artificial intelligence/Machine learning (AI/ML) in the last few years brings considerable progress in the resolution of problems that brings a very great complexity. The methods of ML, especially from deep learning (DL), have proved very effective efficiency in the resolution of problems of very high complexity and the automation of processes in the field of telecommunications. In mobile networks, especially nowadays from 5G, ML/DL is the most suitable technique for process optimization.

Problem statement

In the literature, a huge amount of schemes and algorithms have been proposed for beamforming management in mm-Wave networks. For instance, [Ari et al. \(2019\)](#) proposed a resource allocation scheme for 5G networks that optimally manage the user device and remote radio heads mapping with a low latency and an optimal spectral efficiency. Moreover, [Liu et al. \(2017\)](#) intro-

duced a decentralized beamformer pair scheme based on the game theory. Unfortunately, these mechanisms require a huge amount of iteration and also need a lot of computation resources. Recently, machine learning techniques have been responsible for several performance breakthroughs in many areas including computer vision and data processing. Moreover, machine learning has been applied in solving several challenging problems in telecommunications. The methods enabled a low computational complexity in solving a number of optimization and combinatorial search problems.

Research Objective

Very recently, deep learning that is a special category of machine learning, has been used to optimize wireless communication systems, especially to optimize the beamforming management in mm-Wave networks. By using deep learning mechanism, in-depth patterns hidden in the input data can be abstracted layer by layer. This project aims at proposing a beamforming management (with centralized architecture) mechanism in the context of dense mm-Wave networks by using deep learning.

Construct a model based on DNN used to solve the optimize wireless communication systems, especially to optimize the beamforming management in dense mm-Wave networks.

Organisation of the work

The thesis has four chapters organise as follow: the first chapter is dedicated for an overview of key concepts in 5G mm-Wave, in this we present some main concepts as mm-wave, massive MIMO BM-IC. The second chapter is a survey of existing ML method for BM-IC, in this we present the different ML methods and some previous work on deep learning for BM-IC. The third chapter is dedicated for mm-Wave system modeling, we built the optimization problem related to the model for improve the sum-rate and proposed the approach solution for optimize with DNN and last chapter is dedicated to numerical simulation and results.

1. Overview of key concepts in 5G mobile network

Introduction

The 5th generation network can not be seen as an evolution of previous networks, but rather as a new technological foundation developed to meet the growing bandwidth needs of users [Ari et al. \(2019\)](#). To achieve this goal, 5G is developed based on principles and techniques such as: millimeter-Waves (mm-Waves), massive Multiple-Input and Multiple-Output (MIMO), Beamforming, Small cell, Full duplex, interference management techniques, Inter-Cell Interference Coordination (ICIC) dynamic TDD with self-backhauling and novel access technologies etc [Xiao et al. \(2017\)](#). In this chapter, we present the overview of some main concepts as mm-Waves, Massive MIMO, antenna selection, beam management and interference coordination, used in 5G mobile network.

1.1 Millimeter-Waves

5G use mm-Waves for diffusion, known as Extremely High Frequencies (EHF) or very high frequency (VHF) by the International Telecommunications Union (ITU) to quickly transfer huge amounts of data.

1.1.1 Definition of millimeter waves

mm-Waves can be defined as radio waves covering frequencies from 30 to 300 GHz. Compared to the frequencies below 5 GHz previously used by mobile devices, mm-Waves is a band of radio frequencies that is well suited for 5G networks. These frequencies are called mm-Waves because they have wavelengths between 1 mm and 10 mm, while the wavelengths of the radio waves currently used by smartphones are mostly several dozen centimeters.

1.1.2 Characteristics of mm-Waves

In telecommunications, millimeter waves are used for a variety of services on mobile and wireless networks, as it allows for higher data rates up to 10 Gbps. They have subject to many characteristics that can be advantages or disadvantages. The principal characteristics are:

- wavelengths: mm-Waves have short wavelengths that range from 10 millimeters to 1 millimeter;

- attenuation: mm-Waves have high atmospheric attenuation and are absorbed by gases in the atmosphere, which reduces the range and strength of the waves, mm-waves are subject to rain fade and humidity that can reduce significantly the signal strength;
- Line of Sight (LOS): mm-Waves travel by line of sight, so its high-frequency wavelengths can be blocked by physical objects like buildings and trees.

1.1.3 Capacity Bandwidth in free and non free-space transmission power

mm-Waves are considered as one of the most technologies in 5G mobile network because of the large amount of bandwidth available. Expanding the bandwidth is an efficient approach to enhance system capacity. In particular, the channel capacity of an additive white Gaussian noise channel operating over the bandwidth B is given in Eq. (1.1.1):

$$C = B \log_2 \left(1 + \frac{P}{N_0 B} \right) \quad (1.1.1)$$

where P is the signal power and N_0 is the noise power spectral density [Xiao et al. \(2017\)](#).

According to *Friis transmission formula* [Singh et al. \(2011\)](#), the power of the received signal can be determined by formula given in Eq. (1.1.2):

$$P = P_r = P_t G_t G_r \left(\frac{\lambda}{4\pi} \right)^2 d^{-n} \quad (1.1.2)$$

where P_t is the transmit power and G_t and G_r are the antenna gains of the transmitter and receiver respectively, λ is wavelength, d is the transmission distance, and n the pathloss exponent.

1.1.4 Operating Bandwidth for Wireless communication

High-bandwidth point-to-point communication links are used on mm-Waves ranging from 71 Ghz to 76 Ghz, 81 Ghz to 86 Ghz and 92 Ghz to 95 Ghz announced in 2003 by the Federal Communications Commission (FCC). More recently, in July 2016, FCC dedicated largeband widths in mm-Wave bands for future cut-edge wireless communications, namely 64-71 GHz unlicensed bands (plus previous 57-64 GHz) and 27.5-28.35 and 37-40 GHz licensed bands [Xiao et al. \(2017\)](#).

1.2 Massive MIMO system

In order to ensure the fifth generation objectives for the transmission of digital information at higher speeds and for an increasingly high quality of service, for the resolution network capacity limitation problems in relation to bandwidth or transmission power, 5G uses a new system which is represented by the MIMO Beamforming [Jiang and Kaltenberger \(2018\)](#). This system comprises two technologies, Massive MIMO and Beamforming.

1.2.1 MIMO system

Multiple-Input Multiple-Output (MIMO) technology is based on N_t antennas of transmission and N_r receiving antennas. MIMO can be used to improve the capacity of the channels as well as the channel throughput.

In the case of Fig. 1.1, where we have a MIMO system with N_t transmitters and N_r receivers, the MIMO channel is translated by an H matrix of size $N_t \times N_r$ called channel matrix given in Eq. (1.2.1).

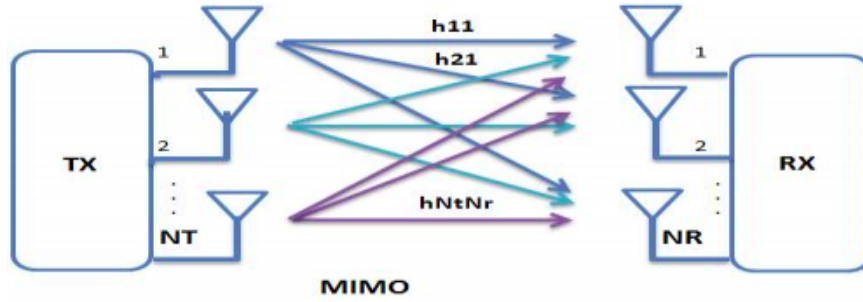


Figure 1.1: MIMO System.

$$H = \begin{pmatrix} h_{11} & h_{12} & \dots & h_{1N_t} \\ h_{21} & h_{22} & h_{23} & \vdots \\ \vdots & \vdots & \ddots & \vdots \\ h_{N_r 1} & h_{N_r 2} & \dots & h_{N_r N_t} \end{pmatrix} \quad (1.2.1)$$

Now, we can define MIMO signal as :

$$Y = HX + n \quad (1.2.2)$$

Where X is a transmitted sequence, Y is a received sequence and n is the noise that corrupts the signal when passing through the channel.

1.2.2 Massive Multi-users MIMO

Massive MIMO is an extension of Multi-Users MIMO (MU-MIMO) [Jiang \(2017\)](#). In this technology, the base station (BS) equipped with many antennas simultaneously serves several users in the same frequency band [Ngo et al. \(2013\)](#). Owing to the large number of degrees-of-freedom available for each user, massive MU-MIMO can provide a very high data rate and communication reliability with simple linear processing such as maximum ratio combining (MRC) or zero-forcing (ZF) on the uplink and maximum-ratio transmission (MRT) or ZF on the downlink [Ngo et al. \(2013\)](#). The fundamental distinctions between massive MU-MIMO and MU-MIMO can be summarized in [ma-mimo.ellintech](#) as follow:

- duplexing mode: conventional MU-MIMO is designed to work with both time-division duplex (TDD) and frequency-division duplex (FDD) operation, when massive MIMO is designed for TDD operation to exploit channel reciprocity;
- channel acquisition: conventional MU-MIMO is mainly based on codebooks with set of predefined angular beams, when massive MIMO is based on sending uplink pilots and exploiting channel reciprocity;
- link quality after precoding/combining: in conventional MU-MIMO, link quality varies over time and frequency, due to frequency-selective and small-scale fading when in massive MIMO there is almost no variations over time and frequency, thanks to channel hardening;
- resource allocation: in conventional MU-MIMO, the allocation must change rapidly to account for channel quality variations when in Massive MIMO, the allocation can be planned in advance since the channel quality varies slowly;
- cell-edge performance: conventional MU-MIMO cell-edge is good only if the BSs cooperate, when the massive MIMO Cell-edge SNR increases proportionally to the number of antennas, without causing more inter-cell interference.

1.2.3 Potentials and characteristics of massive MIMO

1.2.3.1 Potential of Massive MIMO

Massive MIMO technology relies on phase-coherent but computationally very simple processing of signals from all the antennas at the BS [Larsson et al. \(2014\)](#). Some specific benefits of a massive MU-MIMO system are:

- increase of the capacity 10 times or more and simultaneously improve the radiated energy efficiency on the order of 100 times;
- can be built with inexpensive, low power components;
- Enables a significant reduction of latency on the air interface;
- simplifies the multiple access layer;
- increases the robustness against both unintended man-made interference and intentional jamming.

1.2.3.2 Massive MIMO diversity

MIMO diversity is used when the dispersal nature of the channel is used to send multiple replicas of the same signal to the receiver. The more replicas the receiver receives, the less likely it is that all of them will have been highly attenuated, and thus improve the quality of the radio link. The exploitation of channel diversity only serves when the channel is subject to strong attenuation [Roze \(2016\)](#).

1.2.3.3 Temporal diversity

Exploiting the temporal diversity of the channel consists in sending the same signal several times at different times. This is equivalent to distribute the user data over time, e.g., by means of channel coding and time interleaver, in order to be able to recombine in reception, the different instances and reconstruct the useful signal.

Restriction: in order to make the best use of temporal diversity, it is necessary that two instances of the same signal are spaced at least the coherence time (T_{coh}) of the channel, time during which the channel is considered static [Roze \(2016\)](#).

1.2.3.4 Spatial diversity

Space diversity can be exploited when a signal is emitted from several distinct points in space.

Restriction: the distance d in the relation given in Eq. (1.2.3) between each antenna of the same antenna array must be at least half a wavelength for diversity to be exploited (sufficiently decorrelated antennas). Coupling between antennas will also degrade performance.

$$d \geq \frac{\lambda}{2} \quad (1.2.3)$$

1.2.3.5 Spatio-Temporal diversity

Spatial and temporal diversity is an example of a combination of diversity techniques. This technique sends time-delayed versions of the signal via several transmitting antennas. In this way, an easier level of diversity is achieved.

1.2.4 Limitation of massive MIMO

The most limitation of massive MIMO is pilot contamination. In a massive MIMO system, ideally, every terminal is assigned an orthogonal uplink pilot sequence [Larsson et al. \(2014\)](#). The effect of reusing pilots from one cell to another and the associated negative consequences is termed pilot contamination

1.3 Antenna selection

Antenna selection is one of the several techniques using in MIMO system [Khawam et al. \(2016\)](#). However employing more than two transmit antennas impose some constraints of physical limitation of wireless devices. To overcome these problems, while utilizing the advantage of using multiple antennas, several works have appeared recently in the literature in which the notion of

antenna selection was introduced [Dong et al. \(2008\)](#). In this section, we will present the concept and principles of Transmit Antenna Selection with Maximal Ratio Combining (TAS/MRC).

1.3.1 System Model

Let consider the transmit selection antenna of Fig. 1.2 below:

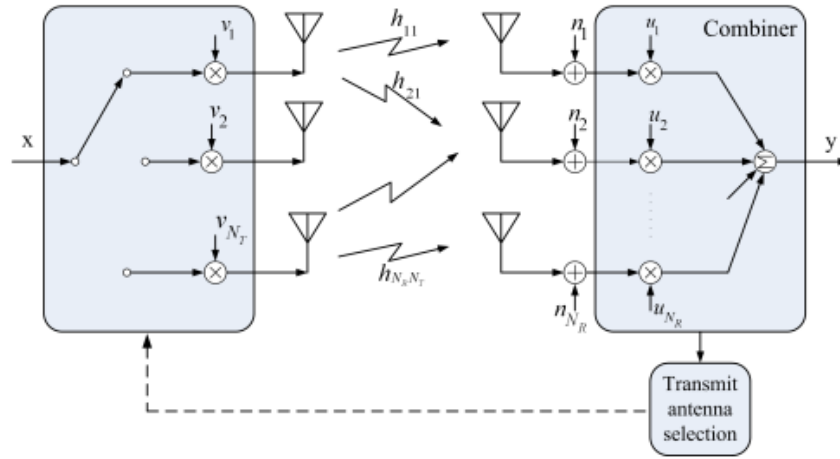


Figure 1.2: Transmit antenna selection with MRC [Dong et al. \(2008\)](#)

Let us consider a narrow-band MIMO communication system with N_T antennas at the transmitter side and N_R antennas at the receiver side, see Fig. 1.1. After antenna selection, K transmit and L receive antennas are used ($K \leq N_T, L \leq N_R$) [Dong et al. \(2008\)](#). The received signals can be written as:

$$y = Hx + n \quad (1.3.1)$$

Where $x = [x_1, x_2, \dots, x_{N_T}]^T$ denotes the transmitted vector, $y = [y_1, y_2, \dots, y_{N_R}]^T$ denotes the received vector and $n = [n_1, n_2, \dots, n_{N_R}]^T$ is a complex additive white Gaussian noise (AWGN) vector with covariance $E\{nn^H\} = N_0 I_{N_R}$, N_0 is the power spectral density of the AWGN at each receive antenna and I_{N_R} denotes the $N_R \times N_R$ identity matrix. We normalize the constellation energy such that $E\{x^H x\} = E_S$, E_S is the total transmit energy. If the antenna elements are closely spaced, and/or the angular spread of the multipath components is small, then the entries of channel matrix are correlated. The $N_R \times N_T$ channel matrix is given below:

$$H = R_{R_x}^{1/2} * H_w * R_{T_x}^{1/2} = \begin{pmatrix} h_{11} & h_{12} & \dots & h_{1N_T} \\ h_{21} & h_{22} & h_{23} & \vdots \\ \vdots & \vdots & \ddots & \vdots \\ h_{N_R1} & h_{N_R2} & \dots & h_{N_R N_T} \end{pmatrix} \quad (1.3.2)$$

Where R_{R_x} and R_{T_x} are the $N_R \times N_R$ receive and $N_T \times N_T$ transmit correlation matrix respectively. H_w is a matrix with independent and identically distributed (iid) Gaussian elements, mean zero and variance unit. The correlation control matrix R , is generated by kronecking the transmit R_{T_x} and the receive R_{R_x} correlation matrix.

$$H = R_{R_x} \otimes R_{T_x} = \begin{pmatrix} 1 & \rho_{12} & \cdots & \rho_{1N_T} \\ \rho_{21} & 1 & \rho_{23} & \vdots \\ \vdots & \vdots & 1 & \vdots \\ \rho_{N_T1} & \rho_{N_T2} & \cdots & 1 \end{pmatrix} \quad (1.3.3)$$

Here $\rho_{i,j}$ are the correlation transmit coefficient (or receive correlation coefficient) between the i^{th} transmit (or receive) antenna and the j^{th} transmit (or receive) antenna.

$\rho_{i,j}$ can be found by the Bessel function $J_0(\delta \frac{2\pi}{\lambda} d(i,j))$ in which Δ is the angle spread, λ is the wavelength, and $d(i,j)$ is the distance from object i to object j , and $J_0(x)$ is the Bessel function of the first kind of the zeroth order [Dong et al. \(2008\)](#)

1.3.2 Optimal antenna subset selection

Let us assume that the channel state information (CSI) is exactly known by the transmitter and the receiver. The selection is based on Signal to Noise Ratio (SNR) at each receive antenna. With the perfect knowledge of the correlation matrix at both sides, the receiver would feedback the choice of active transmit antenna to transmitter. Let consider that K transmit antennas and L received antennas are chosen and all other are inactive. The system can be represented as $(N_T, k; N_R, L)$. We may also use $(N_T; N_R, L)$ or $(N_T, k; N_R)$ to denote the system with antenna selection only at the transmitter or at the receiver.

In case of transmit antenna selection with MRC and $(N_T, k = 1; N_R)$ where $1 \leq i \leq N_R; 1 \leq j \leq N_T$.

$$H = [h_1, h_2, \dots, h_{N_T}] \quad (1.3.4)$$

vector, which is the j^{th} column of H , and is used to denote the channel between the single selected transmit antenna and N_R receive antennas.

$$I = \underset{1 \leq j \leq N_T}{\operatorname{argmax}} \{ \gamma(j) = \frac{E_s}{N_0 N_T} \sum_{i=1}^{N_R} |h_{i,j}|^2 \} \quad (1.3.5)$$

$\gamma(j)$ is the instantaneous SNR of the output of MRC when using transmit antenna j . Through the feedback channel, the value of I is available to the transmitter. The selection criterion of I in Eq. 1.3.5 is to maximize the instantaneous post-processing SNR.

1.4 Beam management and interference coordination

Antenna array is a group of two or more antennas that are integrated together to provide coverage.

1.4.1 Beamforming

Beamforming or spatial filtering is a signal processing techniques used in sensor array for directional signal transmission or reception [Zhou et al. \(2018\)](#).

We have three types of beamforming:

- static beamforming : this performs by using the number of directionnal antennas group together, or sectorial array;
- dynamic beamforming: it focuses the radio frequency (RF) energy in a specific direction and in a particular shape, the radiation pattern of the signal can change on a frame-by-frame basis;
- transmit beamforming : it performs by transmitting multiple phase-shifted, signals will hope that they will arrive in phase at the location of receiver.

1.4.2 Beam management

We can denotes, mm-wave BS as MBS , and mm-wave User Equipment as MUE . Let \mathbb{R}_{MBS} denote the set of MUE_s . Let b_{max} and b_{max}^u denote the maximum beam that the MBS and MUE u can form ($u \in \mathbb{R}_{MBS}$) respectively.

Let $\mathbb{Q} \subseteq \mathbb{R}$ be the set of MUE_s served simultaneously by the MBS and U be the number of MUE_s in \mathbb{Q} , $1 \leq U \leq b_{max}^u$, where $Q = \{MUE_1, MUE_2, \dots, MUE_n\}$ and $|Q| = U$, b and b_u the number of operating beam of the MBS and MUE in initial transmission respectively. Then the numbers of operating beams of the MBS can be expressed as follow:

$$b = \sum_{u \in Q} b_{max}^u \leq b_{max}^{MBS} \text{ where } 1 \leq b_u \leq b_{max}^u.$$

1.4.2.1 Beamspace MU-MIMO

Beamspace MU-MIMO is defined as mm-wave communication mode that an MBS with multiple orthogonal beams can transmit simultaneously to a set of MUE_s where each MUE is one or more operating beams [Xue et al. \(2018\)](#).

If N is the number of pair transmitting and receiving beams between (T-R) (MBS-MUE) then $1 \leq N \leq \min\{b, \sum_{u \in Q} b_u\}$.

1.4.2.2 Beam/user management for Beamspace MU-MIMO

Let consider the Fig. 1.3 which has one omni-directional MBS and two MUE_s :

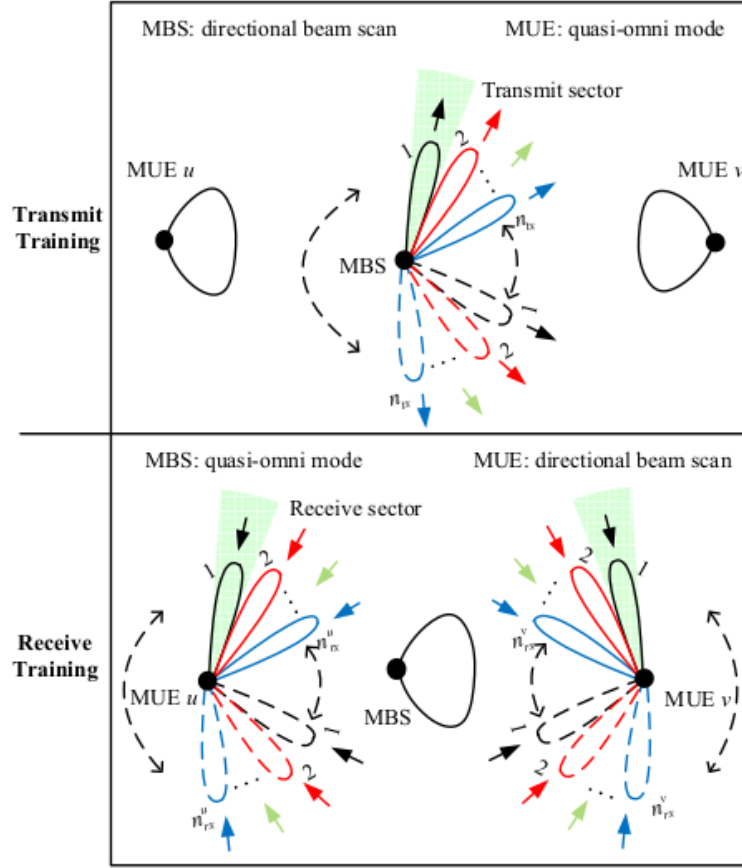


Figure 1.3: Illustration of transmit and receive training for downlink beamspace MU-MIMO Xue et al. (2018)

Fig. 1.3 proposes the schema of multi user BF training mechanism . BF training operations are designed to determine the best Transmit and Receive (T-R) beam $\mathbb{N}_{pair}^u, u \in \mathbb{R}$ pair set that match with LOS/NLOS paths.

This analysis is considered only for downlink performance of Beamspace MU-MIMO Xue et al. (2018).

1.4.2.3 Multi-users Beamforming selection

i) *Transmit training*: in the transmit training phase for beamspace MU-MIMO, the MBS scan n_{tx} transmit sectors quality simultaneously with n_{tx} beams which are mutually orthogonal to each other. All the MUE_s are in the quasi-omni mode. If the total number of transmit sectors is S_{MBS} then we have:

$$1 \leq n_{tx} \leq \min\{b_{max}^{MBS}, S_{MBS}\} \quad (1.4.1)$$

Hence we need to test $\lceil \frac{S_{MBS}}{n_{tx}} \rceil$ times to determine the best set \mathbb{N}_{TX}^u for MUE u ($\forall u \in \mathbb{R}$).

ii) *Receive training*: in the receive training phase for beamspace MU-MIMO, the MUE detect multiple receive sectors quality simultaneously with multiple directional beams which are mutually

orthogonal. All the MBS remains in the quasi-omni mode as MUE at the training. As shown in [Xue et al. \(2018\)](#) we can obtain the best receive beam set \mathbb{N}_{RX}^u after scanning $\lceil \frac{S_u}{n_{rx}^u} \rceil$ times, where S_u is the total number of MUE u 's receive sectors, n_{rx}^u is the number of simultaneous scanning beam, and:

$$1 \leq n_{rx}^u \leq \min\{b_{max}^u, S_u\} \quad (1.4.2)$$

iii) *Beam combining*: the idea is to group in T-R beam candidates which made certain condition of communication require as threshold of SNR (e.g., $SNR \geq \eta$). So after testing beams in transmit \mathbb{N}_{TX}^u and receive \mathbb{N}_{RX}^u set in pairwise, knowing the threshold, we can determine $\mathbb{N}_{pair}^u (\forall u \in \mathbb{R})$ in which there are b_u T-R beams pair candidate $b_u \leq b_{max}^u$. All the selected link qualities of each candidate should meet $SINR_{u,i} \geq \eta (\forall i \in \mathbb{N}_{pair}^u)$.

1.4.3 Interference coordination

The implementation of small size networks delivers various advantages such as high data rate and low signal delay. However, it also suffers from various issues such as inter-cell, intra-cell, and inter-user interferences [Qamar et al. \(2019\)](#). For optimal performance, 5G networks will adopt a more coordinated approach to radio access network (RAN) technology based on Coordinated Multipoint (CoMP) transmission and Inter-cell Interference Coordination (ICIC) and other techniques shown in Fig. 1.4.

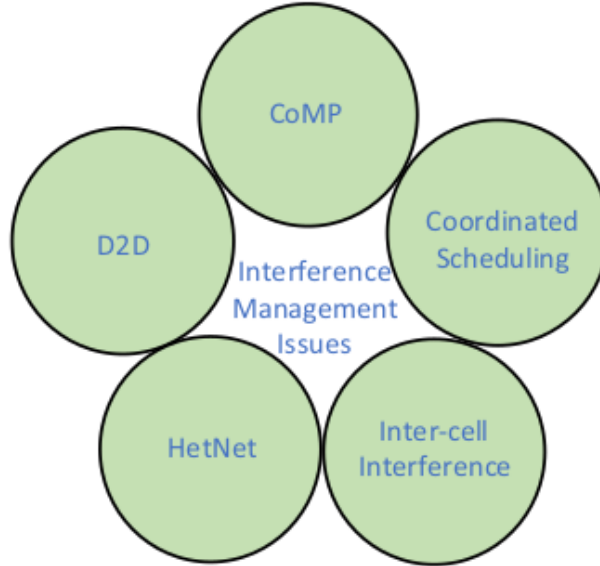


Figure 1.4: 5G interferences management issues [Qamar et al. \(2019\)](#).

1.4.3.1 Coordinated Multipoint

The prime motivation of CoMP as described by 3rd Generation Partnership Project (3GPP) is to improve the coverage, the cell-edge throughput, the overall system throughput. There are two types of CoMP:

- intrasite CoMP: where significant amount of data can be exchanged and doesn't involve the backhaul;
- intersite CoMP: where a single UE can be served by multiple BS of different backhaul technologies in a coordinated manner with less interference.

Two ways in which CoMP operate:

- joint processing, where data is transmitted simultaneously from number of different BSs;
- coordinated Scheduling or Beamforming, data to a single UE is transmitted from one BS.

1.4.3.2 Inter-Cell Interference Coordination

To address the increasing data rate demands for future wireless networks, a dense deployment of BSs or access points is the most promising approach. However, doing so may cause high intercell interference (ICI) [Wang et al. \(2019\)](#). ICI can easily degrade the system's spectral efficiency (SE) and energy efficiency (EE) especially for the cell edge users [Qamar et al. \(2019\)](#). Inter-cell coordination technique such as the ICIC is initially introduced as a solution to ICI in multi-cell networks. ICI technique can be categorized as either static coordination such as ICIC or as dynamic coordination such as the enhanced ICIC (eICIC). ICIC helps to jointly coordinate the transmitted power and resources assignments for both cell-center and cell-edge UEs. Whereas, the eICIC technique, is introduced by 3GPP to minimize the complex coordination overhead experienced in ICIC standard.

Since the quality of different links may vary widely among simultaneous MUEs, we should make a reasonable resources allocation in order to maximize its achievable rate. As shown in [Wang et al. \(2019\)](#) the maximize resource allocation can be obtained by solving Eq. (1.4.3):

$$\begin{aligned}
 & \text{Maximize } \sum_{t \in T} \sum_{n \in N} \sum_{u \in U_n} W_u \sum_{m \in M} r^{u,n,m}(p(t), I(t)) \\
 & \text{Over: } p, I \\
 & \text{subject to :} \\
 & \sum_{u \in U_n} I^{u,n,m}(t) \leq M_{max} \forall n \in N, t \in T \\
 & \sum_{u \in U_n} p^{u,n,m}(t) \leq p^{n,max} \forall n \in N, t \in T
 \end{aligned} \tag{1.4.3}$$

Where W_u is the weight or priority of user u , $(.)^{u,n,m}(t)$ mean that the cell n will transmit to user u using beam m at time t , p is a transmit power, I is the user resource allocated indicator which can take value 1 or 0, T is scheduling period of transmission, N , U are number of cell and users respectively and M is the number of beams in each sector cover the coverage area. we can denote a rate data r as:

$$r^{u,n,m}(p, I) = W \log_2[1 + SINR^{u,n,m}(p, I)] \quad (1.4.4)$$

where W is the bandwidth of the carrier, and $SINR^{u,n,m}$ is the received $SINR$ for user u from cell n on beam m , which is given as follows:

$$SINR^{u,n,m}(p, I) = \frac{g^{u,n} p^{u,n,m}}{\sum_{l \in N, k \in M, (l \neq n \& k \neq m)} I^{u,l,k} * g^{u,l} \times p^{u,l,k} + \sigma^u} \quad (1.4.5)$$

where $g^{u,n}$ is the channel gain between cell n and user u , σ^u is the thermal noise. M_{max} and $p^{n,max}$ are the max number of beams that can be allocated concurrently per cell and the maximum transmit power for cell n respectively.

Conclusion

In this chapter we presented some key concepts as mm-Wave, Massive MIMO, antenna selection, beam management and interference coordination used in 5G mobile network. It appears that the future 5G is a generation of mobile network that brings very high speed and low latency. Also they face some challenges, especially management problems related to the resource allocation that can brought interference's and degrade signal. Some solutions are based on machine learning methods. In the next chapter we will present the Survey of existing Machine Learning based scheme for beam management and interference coordination.

2. Survey of existing Machine Learning based scheme for beam management and interference coordination

Introduction

Over the past few decades, advanced analytics techniques, such as data analytics, data mining, and Machine Learning (ML), have attracted the attention of scientists and industry in various fields in order to exploit very large and diverse data sets. For instance, recently in information communications, a network utilizing big data was demonstrated, and networks and wireless communications that embrace big data have been studied [Joung \(2016\)](#); [Djedouboum et al. \(2018\)](#). In this chapter, we present the ML concept and different works on deep learning for beam management and interference coordination.

2.1 Machine Learning presentation

ML is a field of research that formally focuses on the theory, performance, and properties of learning systems and algorithms. It is a highly interdisciplinary field building upon ideas from many different kinds of fields such as artificial intelligence, optimization theory, information theory, statistics, cognitive science, optimal control, and many other disciplines of science, engineering, and mathematics [Qiu et al. \(2016\)](#). ML is based on specific methods, techniques and algorithms.

2.1.1 General schema for machine learning methods

Fig. [2.1](#) gives the process to follow to consistently achieve results on ML modeling problems.

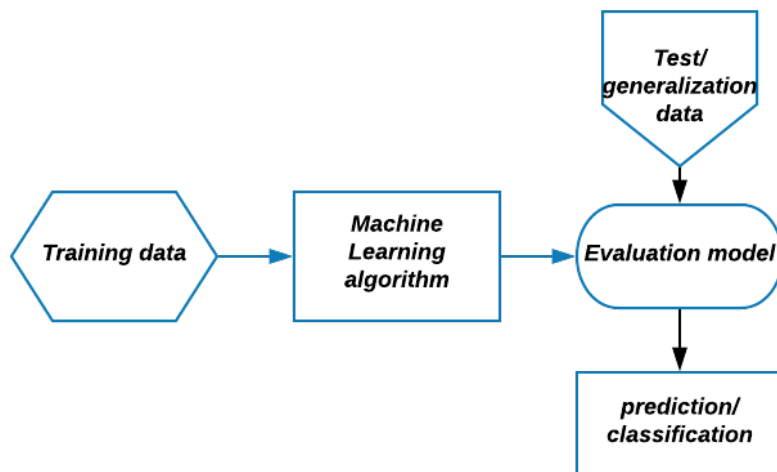


Figure 2.1: Schema for ML methods.

ML process impose to, first of all we have an input data-set that we can divide into training and test sets. We use the training set in step, learning algorithm to train the model, and then in evaluation step we used the test set for evaluating. Then we make a decision.

2.1.2 Machine learning techniques and algorithms

Venn diagram in Fig. 2.2 shows the relation between deep learning, ML, and AI.

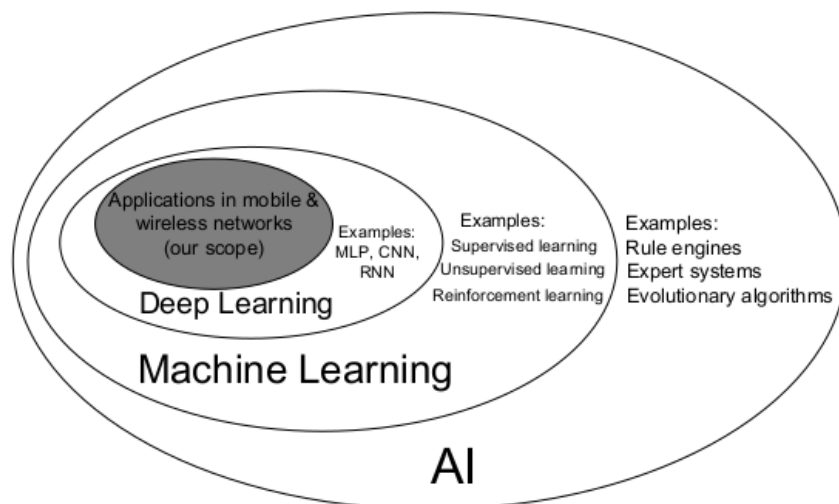


Figure 2.2: Venn diagram of the relation between deep learning, ML, and AI Zhang et al. (2019).

According to this diagram, ML techniques can be naturally categorized into three classes, namely

supervised learning, unsupervised learning, and reinforcement learning. In what follow, our focus is on supervised and unsupervised learning.

2.1.2.1 Supervised learning

In supervised learning, a labeled training set (i.e., predefined inputs and known outputs) is used to build the system model. This model is used to represent the learned relation between the input, output and system parameters. The supervised algorithm are, K-nearest neighbor (k-NN), Decision tree (DT), Support vector machines (SVMs), Bayesian statistics, Neural networks (NNs). Neural networks (NNs) learning algorithm particularly could be constructed by cascading chains of decision units (e.g., perceptrons or radial basis functions) used to recognize non linear and complex functions [Alsheikh et al. \(2014\)](#).

2.1.2.2 Unsupervised learning

Unsupervised learners are not provided with labels (i.e., there is no output vector). Basically, the goal of an unsupervised learning algorithm is to classify the sample set into different groups by investigating the similarity between them. The unsupervised algorithm are, K-means clustering, Principal component analysis (PCA), Reinforcement Learning.

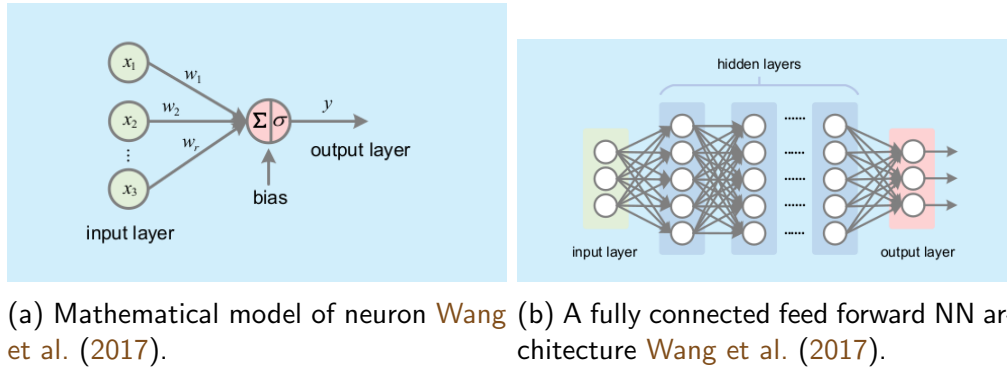
There are particular ML technique like **Deep Learning** that can be both used in supervised or unsupervised Learning .

2.2 Deep Learning

Deep Learning is a set of ML methods attempting to model with a high level of data abstraction through articulated architectures of different non linear transformations. Deep learning algorithms hierarchically extract knowledge from raw data through multiple layers of nonlinear processing units, in order to make predictions or take actions according to some target objective. The most well-known deep learning models are neural networks (NNs), but only NNs that have a sufficient number of hidden layers (usually more than one) can be regarded as 'deep' models [Zhang et al. \(2019\)](#).

2.2.1 Neural Networks

Deep learning is based originally from neural model. That model simulates the biological neural system. The simplest NN is called perceptron, which comprises one input layer and one output layer. Fig. [2.3a](#) called perceptron presents the mathematical model of NN and Fig. [2.3b](#) called multi-layers perceptron (MLP) presents the fully connected feedforward NN architecture where all neurons between adjacent layers are fully connected.



In Fig. 2.3a the weighted sum of several inputs with bias is fed into an activation function $\sigma(\cdot)$ to obtain an output y . An NN is then established by connecting several neuron elements to a layered architecture.

Given an input vector x , a standard MLP layer performs the following operation:

$$y = \sigma(Wx + b) \quad (2.2.1)$$

Here y denotes the output of the layer, W are the weights and b the biases.

2.2.2 Deep Learning activation function

The purpose of an activation function is to add some kind of non-linear property to the function, which is a neural network. Without the activation functions, the only mathematical operation during the forward propagation would be dot-products between an input vector and a weight matrix. Since a single dot product is a linear operation, successive dot products would be nothing more than multiple linear operations repeated one after the other. And successive linear operations can be considered as a one single learn operation. In order to be able to compute really interesting stuff, neural networks must be able to approximate nonlinear relations from input features to output labels. Usually, the more complex the data is, the more non-linear the mapping of features to the ground truth label is.

Increase the number of hidden layers and neurons implies the existence of several other parameters to be determined, thereby making the network implementation difficult. Numerous problems may be encountered during the training process, such as vanishing gradients, slow convergence, and falling into the local minimum. To solve the vanishing gradient problem, new activation functions (e.g., rectified linear units (ReLU), tanh, etc) have been introduced to replace the classic sigmoid function Wang et al. (2017). Table. 2.1 shows some activation functions.

Name	Activation function $\sigma(\cdot)$
sigmoid	$\frac{1}{1+e^{-x}}$
tanh	$\tanh(x)$
softmax	$\frac{e^{x_i}}{\sum_j e^{x_j}}$
ReLu	$\max(0, x)$
Leaky Relu	$\max(0.01x, x)$

Table 2.1: Activation Functions

The use of one or other of these functions depends on the problem we are trying to solve and the value range of the output we are expecting.

A certain loss function, such as square error or cross entropy, must be established for the perceptron to produce a value that is close to the expected one as much as possible. Gradient descent (GD) is commonly used in training the best parameters (i.e., weights and biases) to minimize such loss function.

2.2.3 Deep Learning algorithms

Deep Learning is based on a certain number of algorithms. The most important ones are: Deep Neural Network (DNN), Convolutional Neural Network (CNN), Recurrent Neural Networks (RNNs), Long Short-Term Memory Networks (LSTMs), Deep Boltzmann Machine (DBM), Deep Belief Networks (DBN).

In this part we present three among them , DNN, CNN, RNNs.

i) Deep Neural Networks (DNN)

The DNN uses multiple hidden layers between the input and output layers to extract meaningful features. Fig. 2.3b is an example of DNN.

ii) Convolutional Neural Networks

CNN introduces the idea of designing particular DNN architectures depending on the requirements of specific scenarios. Instead of employing full connections between layers, CNNs employ a set of locally connected kernels (filters) to capture correlations between different data regions Zhang et al. (2019). Fig. 2.4 shows a CNN architecture that adds convolution layers and pooling layers before dense layers.

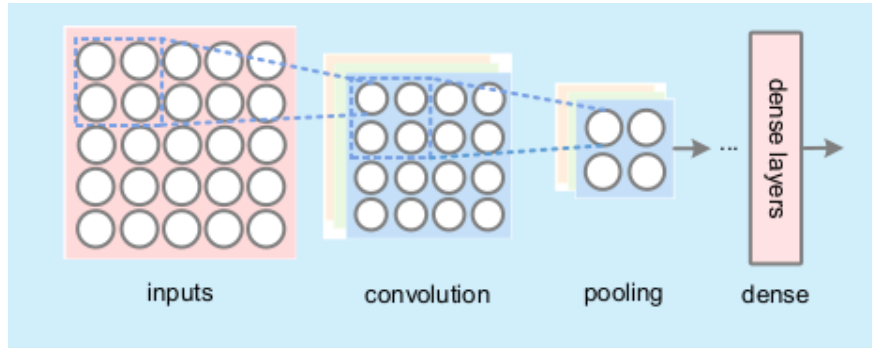


Figure 2.4: A CNN architecture Wang et al. (2017).

Each output in the convolution layers is obtained by dot production between a certain filter matrix and an input matrix is comprised of several neurons in the upper layer. Each output in the pooling layers is obtained by averaging or searching maximum in a group of neurons in the convolution layer.

CNNs improve traditional MLPs by leveraging three important ideas, namely, sparse interactions, parameter sharing, and equivariant representations.

iii) Recurrent Neural Networks

RNNs are designed for modeling sequential data, where sequential correlations exist between samples. At each time step, they produce output via recurrent connections between hidden units, as shown in Fig. 2.5.

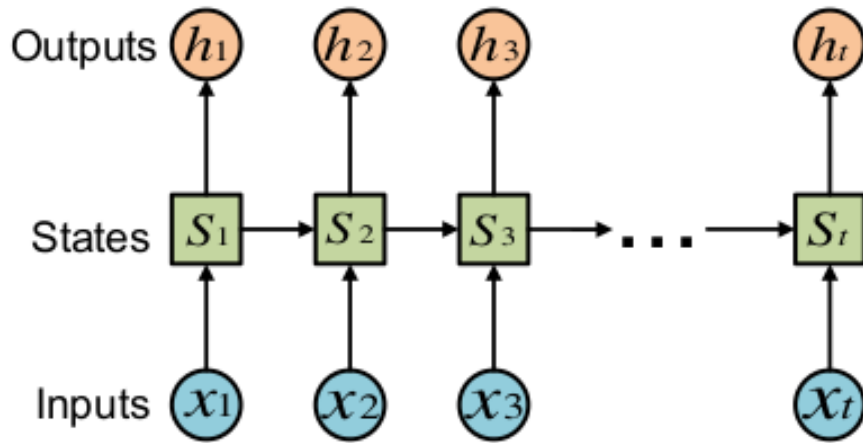


Figure 2.5: A RNN architecture Zhang et al. (2019).

Given a sequence of inputs $x = \{x_1, x_2, \dots, x_T\}$, a standard RNN performs the following operations:

$$\begin{aligned} S_t &= \sigma_s(W_x x_t + W_s S_{t-1} + b_s) \\ h_t &= \sigma_h(W_h S_t + b_h) \end{aligned} \quad (2.2.2)$$

where S_t represents the state of the network at time t and it constructs a memory unit for the network. Its values are computed by a function of the input x_t and previous state S_{t-1} . h_t is the output of the network at time t . The weights W_x, W_h and biases b_s, b_h are shared across different temporal locations. This reduces the model complexity and the degree of overfitting. The RNN is trained via a Backpropagation Through Time (BPTT) algorithm [Zhang et al. \(2019\)](#).

2.3 Insight of Deep Learning based Beam management and interference coordination

Mobile networking and DL problems have been researched mostly independently. Only recently crossovers between the two areas have emerged. Several notable works have been done and are being done coupling the DL and mobile networking research domain.

[Zhou et al. \(2018\)](#) proposed a DNN-based Beam management and interference coordination (BM-IC) method to reduce the interference and improve the sum-rate of dense mm-Wave network. In their work they first proposed an efficient BFT mechanism to establish the directional links between master access point (MAP) and slave access points (SAPs) as well as between access points (APs) and stations (STAs). Secondly, they formulated the BI-MC in dense mm-Wave network as an optimization problem, and then designed a BFT information aided algorithm to generate the training data for DNN-based BM-IC method. The study shows that DNN-based BM-IC can achieve considerable sum-rate with relatively less computing time in dense mm-Wave network, which greatly reduces the overhead for computation ability in actual applications.

[Elbir and Mishra \(2019\)](#) proposed a twin-CNN deep learning approach for joint antenna selection and hybrid beamformer design in mm-Wave communications. In their works they built an optimization problem for the best subarray antenna selection to achieve greater efficiency. They formulated antenna selection and hybrid beamformer design as a classification/prediction problem for CNNs. Instead of computing analog and baseband beamformers, the proposed approach (CNN), does not require the precise knowledge of the channel matrix but only the estimated to feed the network and yields the best antenna subarray and analog and baseband beamformers. The proposed CNN framework improves significantly in the capacity as compared to the conventional beamformer design techniques. They also investigated the quantized-CNN model when it needs to be applied in a low-memory, low-overhead platform such as a mobile phone. They show that at least 5 bits are required for CNN to attain the best subarray and best RF chain performance.

[Alkhateeb et al. \(2018\)](#) proposed a novel integrated communication and machine learning (DL) solution for highly-mobile mm-Wave applications. They formulate the training and design problem of the central baseband and BSs RF beamforming vectors to maximize the system effective achievable rate. The solution considers a low-complexity coordinated beamforming system in which a number of BSs adopting RF beamforming is linked to a central cloud processor applying baseband processing, simultaneously serve a mobile user. Compared to the baseline solution, deep-learning coordinated beamforming achieves a noticeable gain, especially when users are moving with high speed and when the BSs deploy large antenna arrays. The results show that,

for single user learning, coordinated beamforming may not require phase synchronization among the coordinating BSs.

Sim et al. (2020) proposed a deep learning-based beam selection, which is compatible with the 5G NR standard. The paper focus on the initial beam establishment (or beam selection). To select a mm-Wave beam, they exploited sub-6 GHz channel information. They estimate a power delay profile (PDP) of a sub-6 GHz channel, and used as an input of the DNN. By adopting DL for beam selection, time overhead, which will be essential in 5G NR and 6G considerably reduce.

Several of the above mentioned works formulate an optimization problem, which are solved thanks to DL, in a context of distributed architecture and few in centralised architecture but all are applying in a single cell. In this thesis we will investigated how well DL can be used to handle the BF management and interference coordination in 5G mm-wave with centralized architecture in multiple cells.

Conclusion

In this chapter we presented some ML concepts and different works on DL for beam management and interference coordination. It is obvious that ML techniques especially DL algorithms are the most used today in wireless communication systems to improve the latency and ensure higher data rate and quality of services (QoS). However, each system solved with DL has its specificity. The next chapter is dedicated for 5G mm-Wave systems modeling and beamforming mechanism based on Deep Learning.

3. 5G mm-Wave systems modeling and beamforming mechanism based on Deep Learning

Introduction

In this chapter, the main goal is to build the BM-IC model in dense mm-Wave that can help us to generate the SNR data for DL process. In order to achieve this goal, we will first proposed the dense mm-Wave architecture and BFT mechanism, secondly we will build an optimization problem related to the model to improve the overall system sum-rate and proposed the approach solution thirdly we will build a DNN system model for optimization.

3.1 System model for mm-Wave massive MIMO system

In all what follow we will denote by: MAP the master access point, SAP the access point, STA the user equipment. Fig. 3.1 below is the System model of Dense mm-Wave adopted.

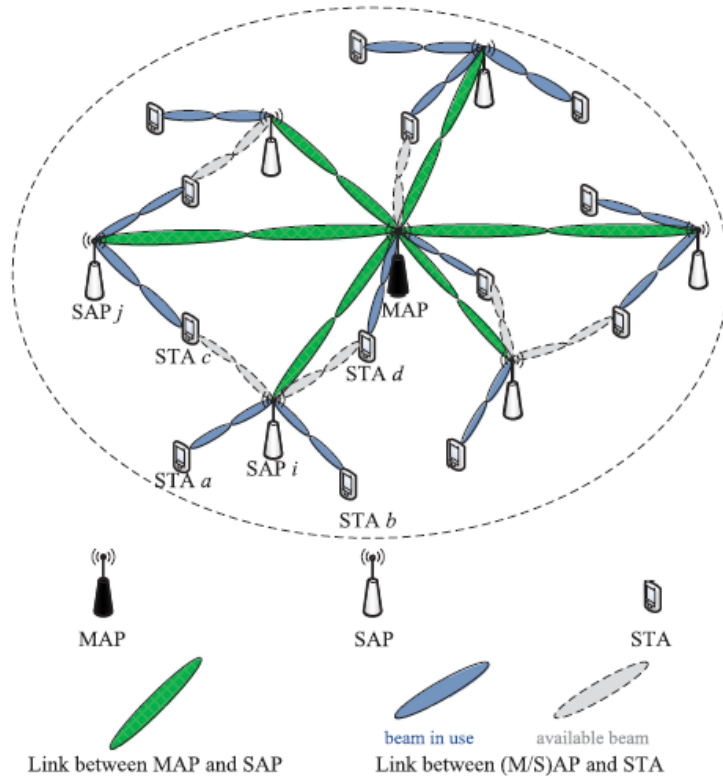


Figure 3.1: Dense mm-Wave network architecture. (Zhou et al., 2018)

The proposed architecture has n $SAPs$, one MAP and s $STAs$. $\mathbb{N} = \{MAP, SAP_1, \dots, SAP_i, \dots, SAP_n\}$ denote the set of $n+1$ APs and $\mathbb{S} = \{STA_1, STA_2, \dots, STA_j, \dots, STA_s\}$ the set of s $STAs$. We assume that all the $SAPs$ are within the MAP 's signal coverage and controlled by the MAP through directional link.

We approximated the antenna as ideal sector antenna model and adopted the normalised directivity gain here the beamforming gain G can be expressed in ? as:

$$G(\alpha, \theta) = \begin{cases} \frac{2\pi - (2\pi - \alpha)\epsilon}{\alpha} & \text{if } |\theta| \leq \frac{\alpha}{2}, \\ \epsilon & \text{Otherwise.} \end{cases} \quad (3.1.1)$$

Where α is the beamwidth of the mainlobe in radian, θ is the beam offset angle to the main lobe in radian, ϵ is the gain of the sidelobe and $0 < \epsilon \leq 1$.

We assume that each beam cover a uniq STA direction in a non overlapping way. Then maximum number of beams of each APs and $STAs$ could be $b_{AP} = \frac{2\pi}{\alpha_{AP}}$ and $b_{AP} = \frac{2\pi}{\alpha_{STA}}$ respectively, where α_{AP} and α_{STA} are the beamwidths of the APs and $STAs$ respectively.

3.1.1 Efficient Beamforming training mechanism for dense mm-Wave network

Figure. 3.2 presents the two steps beamforming training (BFT) mechanism between MAP , $SAPs$ and STA . This training is done in order to allow STA to select the best AP for connecting among all the APs in its area of coverage in term of smaller interference.

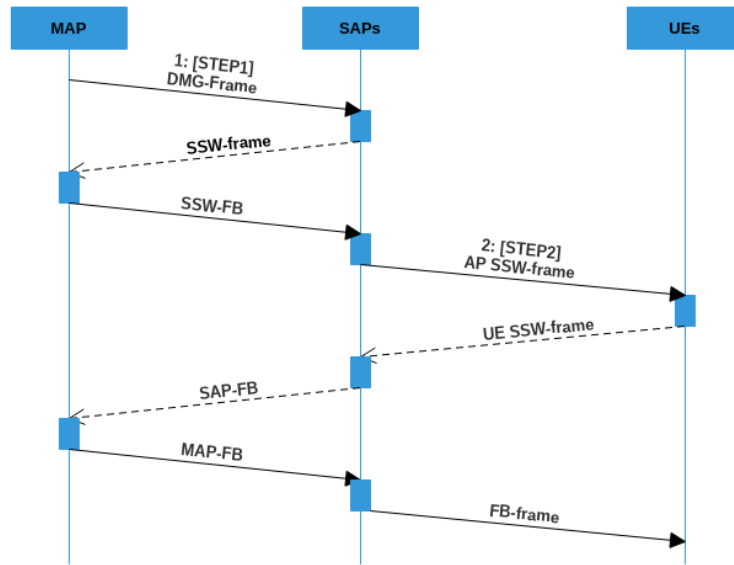


Figure 3.2: BFT mechanism in dense mm-Wave.

3.1.1.1 STEP1: BFT between MAP and SAPs

1. *MAP* transmit directional multi-gigabit (DMG) Beacon frames in all its beams to perform initiator sector sweep (ISS).
2. Each *SAP* selects a training slot to perform responder sector sweep (RSS) by transmitting sector sweep frames in all beams. The training result of ISS are contained in SSW frames.
3. *MAP* transmit SSW-FeedBack (SSW-FB) frames to the *SAPs* which have finished RSS through the best beam indicated in the training results of ISS. The best beam of each *SAP* will be contained in SW-FeedBack frames.

3.1.1.2 STEP2: BFT between APs and STAs

1. Each *AP* transmits SSW frames in all beams to perform BFT of the *AP* side. All the *STAs* at this stage are on quasi-omni listening mode.
2. Each *STAs* selects the training slot to perform BFT in *STAs* side by transmitting SSW frames in all its beams. All the *APs* at this stage are on quasi-omni listening mode.
3. After receiving SSW from *STAs*, each *SAPs* transmits the training results to *MAP* through SAP-FB frame. Then *MAP* can obtain the BFT information of every *STAs*.
4. *MAP* transmits the BFT information of every *STAs* to *SAPs* through MAP-FB frames.
5. Finally, one *SAP* will be selected, based on BFT mechanism information to a transmit FB frame to each *STA*. The FB will inform the *STA*, the best beams between itself and surrounding *APs*.

We assume that we have in the architecture one Master Access point (*MAP*), n slaves access point (*SAPs*) and s stations (*STA*), if denote by b_{AP} and b_{STA} . For the BFT mechanism in IEEE802.11ad/ay denote by equation 3.1.2. In step 1: BFT between *MAP* and *SAP*, *MAP* send to the Access point nb_{AP} beam training frame and the $nSAP$ send back the nb_{AP} response to the *MAP*, the map send n feed-backs to the $nSAP$. So we have for the Step 1: $(b_{AP} + n.b_{AP} + n)$ Step2: BFT between *MAP* and *STA* If we consider only one Access point with all the Station and we proceed the same as above and we have: $(b_{AP} + s.b_{STA} + s)$ considering the n *SAP* and the *MAP* in the network we have $(n + 1)(b_{AP} + s.b_{STA} + s)$ and the IEEE802.11ad/ay is:

$$b_{ad/ay} = (b_{AP} + n.b_{AP} + n) + (b_{AP} + s.b_{STA} + s).(n + 1) \quad (3.1.2)$$

For the dense mm-wave architecture, BFT in Step 1 remain the same as IEEE802.11ad/ay so we have $(b_{AP} + n.b_{AP} + n)$ the beamforming training is assume to be perform one by one by each *AP*, so the have $(n + 1)b_{AP}$ to selected the suitable beam, the *AP* send the feedback to the *MAP* and the response by sending the feedback to the *AP* so we have $2n$ feedback between *MAP* and *SAP* and 1 between *SAP* and the suitable beam selected. This is processed to he s stations in the network. and we have.

$$b_{pro} = (b_{AP} + n.b_{AP} + n) + b_{AP} \cdot (n + 1) + s \cdot (b_{STA} + 2n + 1) \quad (3.1.3)$$

Compared to the BFT mechanism in IEEE802.11ad/ay, the proposed efficient BFT mechanism reduces the BFT overhead. The total number of training frames saved is:

$$b_{save} = b_{ad/ay} - b_{pro} = s \cdot n \cdot (b_{STA} - 1) \quad (3.1.4)$$

3.2 Problem formulation

In the dense mm-Wave network, if the beams between $STAi$ and APj are aligned, according to Eq. 3.1.1, we can obtain the directional transmit gain $G_{i,j}^t$ and received directional receive $G_{i,j}^r$ gain

$$G_{i,j}^t = \frac{2\pi - (2\pi - \alpha_{i,j}^t)\epsilon}{\alpha_{i,j}^t} \quad (3.2.1)$$

$$G_{i,j}^r = \frac{2\pi - (2\pi - \alpha_{i,j}^r)\epsilon}{\alpha_{i,j}^r}, \quad (3.2.2)$$

where $\alpha_{i,j}^t$ is the beamwidth of the transmitter, $\alpha_{i,j}^r$ is the beamwidth of the receiver.

According to Alkhateeb et al. (2018) and Liu et al. (2017), the channel between $STAi$ and APj is given by:

$$h_{i,j}(\tau) = \sum_{k=1}^K G_{i,j}^{(k)t} G_{i,j}^{(k)r} \chi_{i,j}^{(k)c} \delta(\tau - \tau_{i,j}^{(k)}), \quad (3.2.3)$$

where K is the number of paths, and k is the k -th path. $G_{i,j}^{(k)t}$ and $G_{i,j}^{(k)r}$ are directional transmit and receive gain of the k -th path between $STAi$ and APj . $\chi_{i,j}^{(k)c}$ is the amplitude of the k -th path, $\delta(\cdot)$ is the Dirac delta function.

$\tau_{i,j}^{(k)}$ is the propagation delay of the k -th path, $\tau_{i,j}^{(k)} = d_{i,j}^{(k)} / c$, where $d_{i,j}^{(k)} / c$ is the distance of the k -th path between $STAi$ and APj , and c the speed of the light.

We assume the line-of-sight (LoS) path (i.e., $k=1$) always exists Liu et al. (2017), then the rest of the $K - 1$ paths (i.e., $k=2$ to $k=K$) are non-line-of-sight (NLoS). For LoS path, amplitude is given by the following equation Liu et al. (2017):

$$\chi_{i,j}^{(1)c} = \frac{\lambda}{4\pi d_{i,j}^{(1)}}, \quad (3.2.4)$$

Where λ is the wavelength and $\lambda = \frac{c}{f_c}$, f_c is the carrier frequency. $d_{i,j}$ is the distance of LoS path between $STAi$ and APj . For the NLoS paths, $\chi_{i,j}^{(k)}$ include both pathloss and reflection coefficients, and it's given by Liu et al. (2017):

$$\chi_{i,j}^{(k)} = \frac{\lambda}{4\pi d_{i,j}} \prod_{r=1}^R \Gamma_r^{(k)}, k \in [2, K], \quad (3.2.5)$$

Where $\Gamma_r^{(k)}$ is the reflection coefficient of the r -th reflection for k -th path, and R is the number of reflection of the path. Since the reflection loss is very high in mm-wave band, we can consider only one reflection of a given path (i.e. $R=1$). Then, $\chi_{i,j}^{(k)}$ can be rewritten as:

$$\chi_{i,j}^{(k)} = \frac{\lambda}{4\pi d_{i,j}} \Gamma_r^{(k)}, k \in [2, K], \quad (3.2.6)$$

According to Cui et al. (2018), the channel gain can be derived by:

$$G_{i,j}^{(k)} = |\chi_{i,j}^{(k)} \delta(\tau - \tau_{i,j}^{(k)})|^2, \quad (3.2.7)$$

By replacing this expression in Eq. 3.2.3 we can rewritten the channel response $h_{i,j}(\tau)$ as:

$$h_{i,j}(\tau) = \sum_{k=1}^K G_{i,j}^{(k)} G_{i,j}^{(k)} G_{i,j}^{(k)}, \quad (3.2.8)$$

Let denote by $P_{i,j}^t$ the directional beam's transmit power from APj and $STAi$, and $P_{i,j}^r$ the directional beam's received power at the $STAi$ side coming from APj . Then the received power can be determined by:

$$P_{i,j}^r = P_{i,j}^t \sum_{k=1}^K G_{i,j}^{(k)} G_{i,j}^{(k)} G_{i,j}^{(k)}, \quad (3.2.9)$$

Similarly, the interference power received at $STAi$ from another APs (e.g., $b(b \in \mathbb{N} \setminus j)$) and $STAs$ (e.g., $a \in \mathbb{S} \setminus i$) should be:

$$P_{a,b \rightarrow i,j}^I = P_{i,j}^t \sum_{k=1}^K G_{a,b \rightarrow i,j}^{(k)} G_{a,b \rightarrow i,j}^{(k)} G_{i,b}^{(k)}, \quad (3.2.10)$$

Where $G_{a,b \rightarrow i,j}^{(k)}$ and $G_{a,b \rightarrow i,j}^{(k)}$ are directional transmit gain and directional receive gain from the k -path between $STA a$ and $AP b$, respectively. According to Eq. 3.1.1, the directional transmit-receive gain of each path can be derived by:

$$G_{a,b \rightarrow i,j}^t G_{a,b \rightarrow i,j}^r = \begin{cases} \frac{2\pi - (2\pi - \alpha_{i,j}^t)\epsilon}{\alpha_{i,j}^t} \cdot \frac{2\pi - (2\pi - \alpha_{i,j}^r)\epsilon}{\alpha_{i,j}^r} & \text{if } |\theta_{a,b \rightarrow i,j}^t| \leq \frac{\alpha_{i,j}^t}{2} \\ \text{and } |\theta_{a,b \rightarrow i,j}^r| \leq \frac{\alpha_{i,j}^r}{2}, \\ \frac{2\pi - (2\pi - \alpha_{i,j}^t)\epsilon}{\alpha_{i,j}^t} \cdot \epsilon & \text{if } |\theta_{a,b \rightarrow i,j}^t| \leq \frac{\alpha_{i,j}^t}{2} \\ \text{and } |\theta_{a,b \rightarrow i,j}^r| > \frac{\alpha_{i,j}^r}{2}, \\ \epsilon \cdot \frac{2\pi - (2\pi - \alpha_{i,j}^r)\epsilon}{\alpha_{i,j}^r} & \text{if } |\theta_{a,b \rightarrow i,j}^t| > \frac{\alpha_{i,j}^t}{2} \\ \text{and } |\theta_{a,b \rightarrow i,j}^r| \leq \frac{\alpha_{i,j}^r}{2}, \\ \epsilon \cdot \epsilon & \text{if } |\theta_{a,b \rightarrow i,j}^t| > \frac{\alpha_{i,j}^t}{2} \\ \text{and } |\theta_{a,b \rightarrow i,j}^r| > \frac{\alpha_{i,j}^r}{2}. \end{cases} \quad (3.2.11)$$

Where $\theta_{a,b \rightarrow i,j}^t$ and $\theta_{i,j \rightarrow a,b}^r$ are the beam's offset angles from AP b 's (AP b transmits to $STAi$ a) transmit beam direction to the position of $STAi$ and from the $STAi$'s ($STAi$ receives from APj) receive beam direction to the position of AP b , respectively.

We suppose that $STAi$ cannot support multiple connectivity so it can connect only on one AP at a time in the network. Let define a binary variable x .

$$x_{i,j} = \begin{cases} 1 & \text{if } STAi(i \in \mathbb{S}) \text{ is connected to } APj(j \in \mathbb{N}), \\ 0 & \text{Otherwise.} \end{cases} \quad (3.2.12)$$

When $STAi$ is connected to the APj according to Eq. 3.2.9 and Eq. 3.2.10 the $SINR$ between APj and $STAi$ is written as:

$$SINR_{i,j} = \frac{x_{i,j} P_{i,j}^r}{\sum_{a \in \mathbb{S} \setminus i} \sum_{b \in \mathbb{N} \setminus j} x_{a,b} P_{a,b \rightarrow i,j}^I + W \cdot N_0} \quad (3.2.13)$$

where W and N_0 represent the bandwidth of mm-Wave band and the background noise power spectrum density, respectively.

Then, the sum-rate of the entire mm-Wave network is:

$$T = \sum_{i \in \mathbb{S}} \sum_{j \in \mathbb{N}} x_{i,j} W \log_2(1 + SINR_{i,j}) \quad (3.2.14)$$

In other to maximize the sum-rate of the entire mm-Wave network, the BM-IC problem can be transformed into the following optimization problem:

$$\begin{aligned}
 P_1 : & \underset{X, P, A}{\text{Maximize}} \sum_{i \in \mathbb{S}} \sum_{j \in \mathbb{N}} x_{i,j} W \log_2(1 + SINR_{i,j}) \\
 & \text{subject to :} \\
 & C_1 : x_{i,j} = 0, 1, \forall i \in \mathbb{S}, j \in \mathbb{N}, \\
 & C_2 : \sum_{j \in \mathbb{N}} x_{i,j} \leq 1, \forall i \in \mathbb{S}, \\
 & C_3 : \sum_{i \in \mathbb{S}} x_{i,j} \leq b_{AP}, \forall j \in \mathbb{N}, \\
 & C_4 : \sum_{i \in \mathbb{S}} x_{i,j} P_{i,j} \leq p_j^{max}, \forall j \in \mathbb{N}, \\
 & C_5 : \alpha^{min} \leq \alpha_{i,j} \leq \alpha^{max}, \forall i \in \mathbb{S}, j \in \mathbb{N}, \\
 & C_6 : \sum_{i \in \mathbb{S}} x_{i,j} \alpha_{i,j} \leq 2\pi, \forall j \in \mathbb{N},
 \end{aligned} \tag{3.2.15}$$

Where X , A and P are the matrices with element $X_{i,j}$, $P_{i,j}^t$ and $\alpha_{i,j}$ respectively. Constraint C_2 ensures that each STA can connect only on one AP . Constraint C_3 indicates that the number of STA that one AP can serve is always less or equal than b_{AP} . Constraint C_4 is the power consumption of each AP that cannot exceed P^{max} . Constraint C_5 is for the beamwidth limitation between $[\alpha^{min}, \alpha^{max}]$ and C_6 is used to ensure that the sum of beamwidths used for serving connected $STAs$ cannot exceed 2π . The optimization problem P_1 is an NP-hard and non convex problem, and cannot be solved directly. Thus needs some considerations to be solved.

3.3 Beam management and interference coordination in Dense mm-Wave network

3.3.1 Beamforming Training Information Aided Beam Management and Interference Coordination

Since the pathloss of mm-Wave band is serious and the transmit power is limited in practical scenarios, an STA may not receive from all the APs in the network. Thus, an STA can only connect to its available surrounding APs . Each AP can get a candidate STA set based on the BFT results. Assume the candidate STA set of $APj(j \in \mathbb{N})$ is $\mathbb{S}_j(\mathbb{S}_j \subseteq \mathbb{S})$, then the directional link's quality ($SINR_{i,j}$) between $STAi(i \in \mathbb{S}_j)$ and APj should be greater than a predefined threshold $SINR^{pre}$. Therefore, problem P_1 can be rewritten as:

$$\begin{aligned}
 P_2 : \text{Maximize}_{X,P,A} & \sum_{i \in \mathbb{S}} \sum_{j \in \mathbb{N}} x_{i,j} W \log_2(1 + SINR_{i,j}) \\
 \text{subject to :} & \\
 C_1 : & x_{i,j} = 0, 1, \forall i \in \mathbb{S}_j, j \in \mathbb{N}, \\
 C_2 : & \sum_{j \in \mathbb{N}} x_{i,j} \leq 1, \forall i \in \mathbb{S}, \\
 C_3 : & \sum_{i \in \mathbb{S}_j} x_{i,j} \leq b_{AP}, \forall j \in \mathbb{N}, \\
 C_4 : & \sum_{i \in \mathbb{S}_j} x_{i,j} P_{i,j} \leq p_j^{max}, \forall j \in \mathbb{N}, \\
 C_5 : & \alpha^{min} \leq \alpha_{i,j} \leq \alpha^{max}, \forall i \in \mathbb{S}_j, j \in \mathbb{N}, \\
 C_6 : & \sum_{i \in \mathbb{S}_j} x_{i,j} \alpha_{i,j} \leq 2\pi, \forall j \in \mathbb{N},
 \end{aligned} \tag{3.3.1}$$

It is noteworthy that MAP can obtain all the signal-noise-ratio ($SINR$) values (*i.e.*, $SINR_{i,j}$ ($i \in \mathbb{S}_j, j \in \mathbb{N}$)) when BFT is done. For the sake of simplicity of analysis, we store all the $SINR$ values into $\mathbb{Z} = \{z_1, \dots, z_k, \dots, z_K\}$ in descending order. Then, there is a one-to-one match between elements z_k ($k = 1, 2, \dots, K$) and $SINR_{i,j}$ ($i \in \mathbb{S}_j, j \in \mathbb{N}$), where $K = \sum_{j \in \mathbb{N}} Card(\mathbb{S}_j)$, $Card(.)$ stands for the number of elements in a set. Since there are $Card(\mathbb{S}_j)$ candidate STAs for AP_j , there will be $Card(\mathbb{S}_j)$ $SINR$ values for AP_j when BFT is done. For all the $AP_s \in \mathbb{N}$, there will be $\sum_{j \in \mathbb{N}} Card(\mathbb{S}_j)$ $SINR$ values in total. In addition, the number of elements in X, P and A is also $\sum_{j \in \mathbb{N}} Card(\mathbb{S}_j)$. Since problem P_2 is also NP-hard and not convex, it cannot be solved directly neither.

3.3.2 The proposed approach solution of problem P2

The proposed solution for problem **P2**, presented in **Algorithm 1** used a **block coordinate descent method** to solve the Problem Bertsekas and Tsitsiklis. The method consist of each time optimizing one set of variable while keeping the rest fixed. The propose approach solution algorithm decompose problem P_2 into three sub-problems to find the sub-optimal solution, *i.e.*:

1. initialize P and A to obtain the optimized X^* ;
2. use the optimized X^* and initialized P to get the optimized A^* ;
3. use the optimized X^* and A^* to find the optimized P^* .

Algorithm 1 P2 Beamforming Training Aided solution

Initialize $X = \{0\}$, $A = \{\alpha^{max}\}$, $X = \{P^{max}/b_{AP}\}$;
 Compute the different $SNR_{i,j}$ values with the formula $SNR_{i,j} = \frac{P_{i,j}^r}{W \cdot N_0}$ and Store the value into a vector $\mathbb{Z} = \{z_1, \dots, z_k, \dots, z_K\}$;
 $z_k \leftarrow SNR_{i,j}$, where $K = \sum_{j \in \mathbb{N}} Card(\mathbb{S}_j)$;
 $k = 1$, compute $T_k = W \log_2(1 + SNR_{i,j})$, set $x_k = 1$;
repeat
 $k = k + 1$, compute T_k ;
 if $T_k > T_{k-1}$ **then**
 set $x_k = 1$;
 else
 set $x_k = 0$;
 end if
until $k = K$
 Obtain $X^* \leftarrow \{x_1, \dots, x_k, \dots, x_K\}$
 compute $SINR_{i,j} = \frac{x_{i,j} P_{i,j}^r}{\sum_{a \in \mathbb{S} \setminus i} \sum_{b \in \mathbb{N} \setminus j} x_{a,b} P_{a,b \rightarrow i,j}^I + W \cdot N_0}$ by adopting X^* and P Store the value into a vector $\mathbb{Z}^{(1)} = \{z_1, \dots, z_q, \dots, z_Q\}$;
 $z_q \leftarrow SINR_{i,j}$, where $Q = \sum_{x_k \in X^*} x_k$;
 $\alpha_q \leftarrow \alpha^{min}, \alpha, \alpha^{max}$
 $q = 1$, compute $T_q = W \log_2(1 + SINR_{i,j})$, set $x_q = \alpha^{max}$;
repeat
 $q = q + 1$, compute T_q ;
 if $T_q > T_{q-1}$ **then**
 $\alpha_q = \alpha^{max}$;
 if $T_q = T_{q-1}$ **then**
 $\alpha_q = \alpha$;
 else
 $\alpha_q = \alpha$;
 end if
 end if
until $q = Q$
 Obtain $A^* \leftarrow \{\alpha_1, \dots, \alpha_k, \dots, \alpha_K\}$;
 compute optimized P^* using X^* and A^* in weighted minimum mean square error ;
 Output X^* , P^* and A^* .

As shown in algorithm **Algorithm 1** to obtain the optimized X^* , we first initialize the power allocation of each transmit beam as a vector P , which value are the average power allocation of each beam, we initialise the beamwith as a vector of value maximum beamwith, after that we initialise X to zero. Secondly we compute the $SNR_{i,j}$ values of pair AP_j and STA_i and store into vector $\mathbb{Z} = \{z_1, \dots, z_k, \dots, z_K\}$. Then compute the sum-rate T_1 for $k = 1$ and set $x_1 = 1$ and for all the rest of z_k value in a list, if $T_k > T_{k-1}$ set $x_k = 1$; otherwise set $x_k = 0$. After

mapping x_k to $x_{i,j}$ we obtained the optimized X^* . Each value in X^* indicates the beam direction and which AP each STA should connect to. After determining X^* we used it to find the optimal A^* . For that we used the optimized X^* and average power allocation P , compute the $SINR_{i,j}$ values using equation. 3.2.13 and stored the values in $\mathbb{Z}^{(1)} = \{z_1, \dots, z_q, \dots, z_Q\}$. For each value in \mathbb{Z} compute T_q and set beamwidth value as shown in **Algorithm 1**. So after mapping α_k with $\alpha_{i,j}$ we get the optimized beamwidth A^* . Then, the optimized P^* obtained by using X^* and A^* with the formula:

$$P = 10^{\frac{SINR}{10}} \quad (3.3.2)$$

3.4 Deep Learning based Beam Management and Interference Coordination

3.4.1 System Setup

According to Lee et al. (2018) problem P2 can be assimilated as a linear sub-assignment problems (LSAP) which can be solved by DNN. The basic idea of LSAP is the decomposition of a problem into n sub-assignment problems. Therefore P2 can be decomposed into three sub-assignment problems. Figure. 3.3 presents the system model of DNN based LSAP.

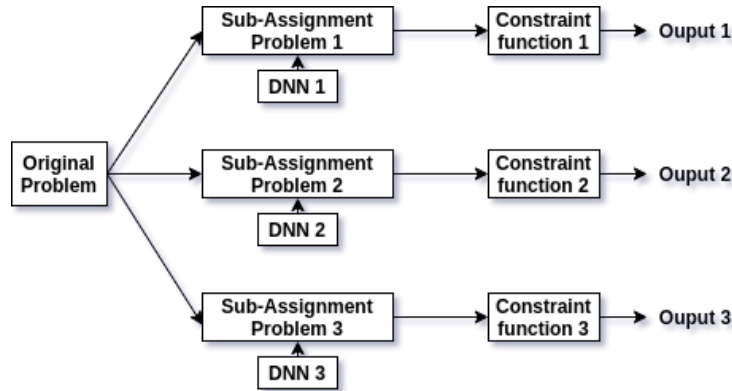


Figure 3.3: System model of DNN based LSAP

The architecture of the learning based approach for LSAP is illustrated in Figure. 3.3. The original problem in our case is the maximization of sum-rate in dense mm-wave network. The sub-assignment problem here consists of finding the optimal AP and the STA which should be connected on, the beamwidth and power allocation of a specific beam. The constraint function help to evaluate the Mean square error (MSE). Our system model based on DNN has three parts, the upper part is used for obtaining the X^* , the middle part for obtaining the A^* and the lower part for obtaining P^* .

3.4.2 DNN structure

The Figure. 3.4 shows the DNN structure used.

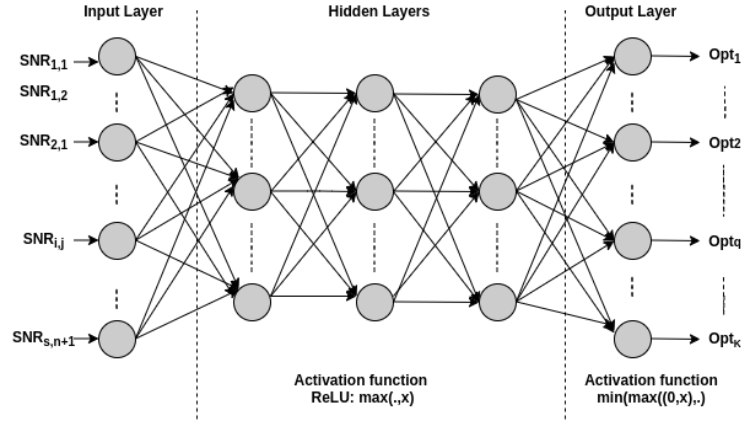


Figure 3.4: DNN structure for j -th sub-assignment problem.

The proposed approach here uses a fully connected neural network with one input layer, three hidden layers, and one output layer as shown in Figure. 3.4. The input of the three parts are the $\{SNR_{i,j}\}$ values generated in **Algorithm 1**. Since we have s STA and $n + 1$ APs the input layer size is $s.(n + 1)$. We use rectified linear unit (ReLU) for the hidden layers activation of the three parts because ReLU can improve the training efficiency by mapping negative values to zero and keeping positive values. In order to enforce the different constraints in the different sub-problem we define a special activation function adapted for each problem shown in equation Eq. 3.4.1, Eq. 3.4.2, Eq. 3.4.3 and Eq. 3.4.4. The ReLU activation function in hidden layers can be defined mathematically by:

$$ReLU = \max(., x) \quad (3.4.1)$$

In the upper part activation function of the output layers with respect of the condition that, each STA can connect to one AP is given by:

$$y_{upper} = \min(\max(0, x), 1) \quad (3.4.2)$$

Where we limit the x_k either to 0 or 1.

In order to limit the beamwidth to $[\alpha^{min}, \alpha^{max}]$ we adopt Eq. 3.4.2 as the activation function for the output of the middle part given by:

$$y_{middle} = \min(\max(\alpha^{min}, x), \alpha^{max}) \quad (3.4.3)$$

Similarly to satisfy the constraint of the power allocation ($0 \leq p_k \leq P^{max}$) in the lower part we can define:

$$y_{lower} = \min(\max(0, x), P^{max}) \quad (3.4.4)$$

3.4.3 Data Generation

The data is generated in the following manner. First, to generate the SNR values, we let the $n+1$ AP s uniformly distributed in the network and fix the distance between two adjacent AP s, we assume that the s $STAs$ are uniformly and randomly distributed in the network. So we randomly generated the distance between AP_j and STA_i , we used the Eq. 3.4.5 to obtain the different $SNR_{i,j}$ values.

$$SNR_{i,j} = \frac{x_{i,j} P_{i,j}^r}{W \cdot N_0} \quad (3.4.5)$$

The entire $SNR_{i,j}$ values obtained in Eq. 3.4.5 used as input of **Algorithm 1**, then we obtained the optimized $\{x_k\}$, $\{\alpha_k\}$ and $\{p_k\}$ from the output. Then we repeated the above process for multiple times to generate the entire training data set with different topology of network, as well as the validation data set denoted by $(T_{\Delta}, T_{\square}, T_{\nabla})$ and $(V_{\Delta}, V_{\square}, V_{\nabla})$ respectively. The input-output pair of $\{SNR_{i,j}, x_k\}$ in T_{Δ} are used to train the upper part of **DNN**. The middle part of **DNN** can be trained by the input-output $\{SNR_{i,j}, \alpha_k\}$ in T_{\square} and the lower part by the input-output $\{SNR_{i,j}, p_k\}$ in T_{∇} . We used the same method for testing set generation with more less computation time.

3.4.4 Training stage

We use the entire training data set coming from T_{Δ} to train the upper part of **DNN** structure. The cost function we use is the mean squared error between the label optimized X^* and the output of the upper **DNN** denoted by X^{DNN} , the cost function is given by:

$$L_{\Delta} = \sqrt{\|X^* - X^{DNN}\|} \quad (3.4.6)$$

For the middle part we used the T_{\square} training set the cost function defined by:

$$L_{\square} = \sqrt{\|A^* - A^{DNN}\|} \quad (3.4.7)$$

Where A^* is the output of **Algorithm 1** and A^{DNN} is the output of the middle part.

As for the upper and middle part, the lower part used the training dataset T_{∇} and the cost function used is the mean square error between P^* and P^{DNN} , given by:

$$L_{\nabla} = \sqrt{\|P^* - P^{DNN}\|} \quad (3.4.8)$$

3.4.5 Testing stage

At the testing stage, we used the data $(V_{\Delta}, V_{\square}, V_{\nabla})$ generated with **Algorithm 1** in Data Generation stage.

Conclusion

In this chapter we modelled a BM-IC problem which is the NP hard optimization problem. We used the **block coordinate descent method** to find the approach solution with **Algorithm 1**, and then we generated the data that can be used in DNN model. We proposed the DNN model for optimizing BM in dense mm-wave network. In the next chapter we are going to present the numerical simulation results of each step of modelled problem.

4. Numerical Simulation and Performance evaluation

Introduction

In this chapter we present the numerical results obtained in BFT mechanism process and in DNN process.

4.1 The performance of efficient Beamforming Training Mechanism

The simulation in this part has been done with MATLAB.

4.1.1 Evaluation of the impact of the number of AP and STA

Here the analysis considers the numbers of training frames as the overhead of BFT. For the simulation we assumed that AP and STA has the same beamwidth ($\alpha_{AP} = \alpha_{STA} = 10^\circ$) and the AP ranges from 1 to 10, the STA ranges from 1 to 100. Using the BFT overhead formula of IEEE802.11ad/ay in Eq. 3.1.2 we get the Figure. 4.1.

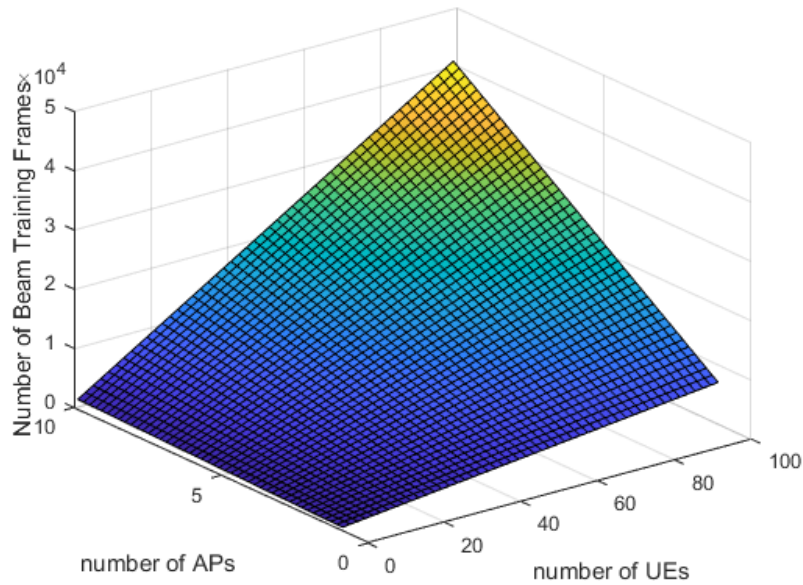


Figure 4.1: The overhead of IEEE802.11ad/ay BFT.

We can see that when we increase the numbers of AP or the number of STA the overhead of BFT also increase.

For proposed BFT mechanism we used Eq. 3.1.3 and get the Figure. 4.2.

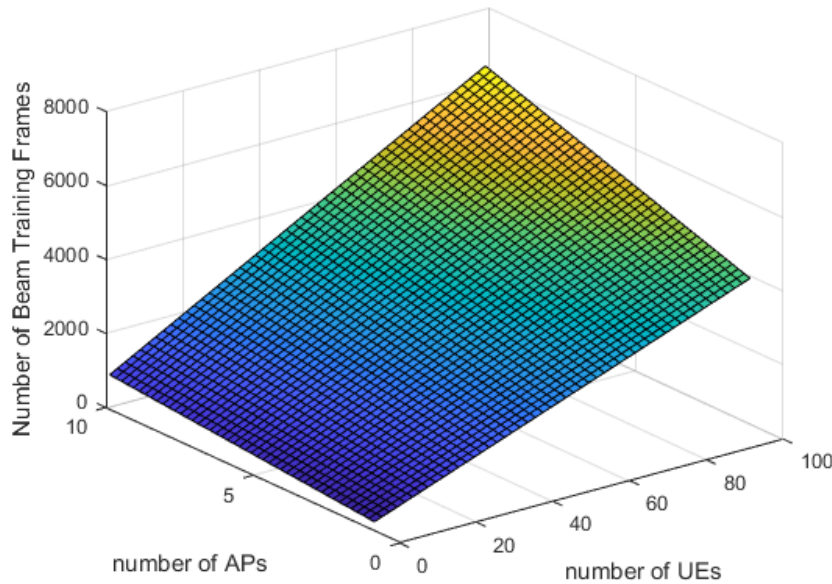


Figure 4.2: The overhead of proposed BFT mechanism.

We can see that the overhead decreases significantly. For the same number of AP and STA (10 and 100) respectively, we have for IEEE802.11ad/ay, 4.5×10^4 beam training frames where the proposed BFT gives 0.6×10^4 beam training frame. We can deduce that the proposed BFT mechanism reduces the overhead at around 15% compared to the IEEE802.11ad/ay BFT. We can conclude that the larger the numbers of APs and $STAs$ is, the more obvious the proposed BFT mechanism will be.

4.1.2 Evaluation of the impact of the beamwidth

For the beamwidth impact evaluation, we fix the number of APs and $STAs$ to 10 and 100 respectively. We considered the beamwidth of APs and $STAs$ equals ($\alpha_{AP} = \alpha_{STA}$) and they take value from $\{10^\circ, 20^\circ, 30^\circ, 45^\circ, 60^\circ\}$, respectively. Figure. 4.3 shows the performance comparison between the BFT in IEEE802.11ad/ay and proposed BFT mechanism.

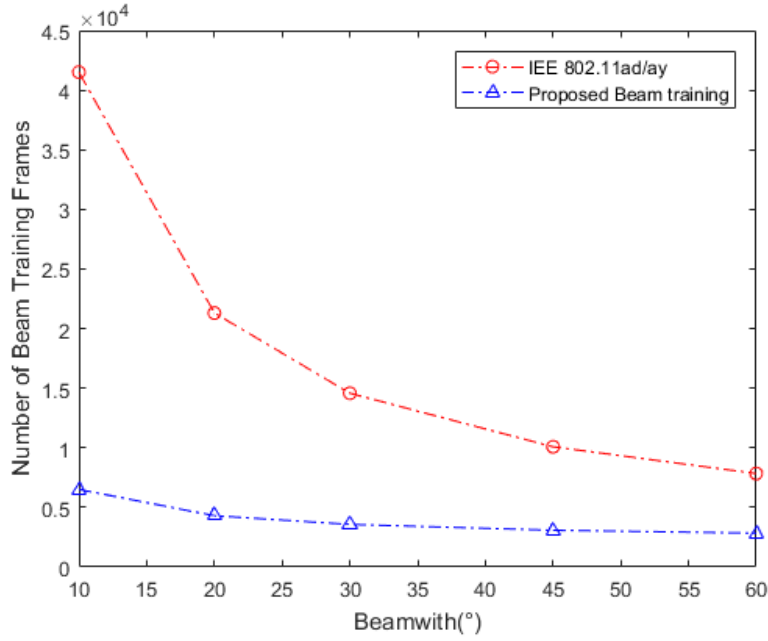


Figure 4.3: The performance between BFT in IEEE802.11ad/ay and proposed efficient BFT mechanism

We can see that when the beamwidth is 10° we have 0.5×10^4 as in Figure. 4.1 and Figure. 4.2 for proposed BFT mechanism. We can observe in this figure that when the beamwidth increases the numbers of beamframes become stable at around 0.3×10^4 . we can also see that the proposed BFT mechanism reduces the number of beamwidth compared to the overhead of IEEE802.11ad/ay. Based on this we can conclude that the proposed BFT mechanism reduces the overhead in dense mm-wave network.

4.2 The performance of Deep Learning Based Beam Management

4.2.1 Simulation setup

In the table. 4.1, we listed the parameters used in **Algorithm 1** to generate the SNR values and the different training and testing data set.

Parameters	Values
Carrier frequency: f_c	60 GHz
Bandwith: W	2.16 GHz
Maximum nubmber of path: K	3
Reflection coefficient: Γ	0.3
Maximum transmit power: P^{max}	43 dBm
Background noise power spectrum density: N_0	-174dBm/Hz
Beamwith: α	$10^\circ, 20^\circ, 30^\circ$
The side lobe gain: ϵ	0.01
Training data set: $(T_\Delta, T_\square, T_\nabla)$	20000
Testing data set: $(V_\Delta, V_\square, V_\nabla)$	5000

Table 4.1: Simulation parameters

As mentioned in Data Generation stage we choose differents configurations of the network(numbers of APs and $STAs$ in the network) and we fix the distance between two adjacents APs . We randomly generated the distances between AP_j and STA_i , we made that process 20000 times to get to 20000 differents networks topology which results to the input SNR Data Frame shown in Figure. 4.4.

	z0	z1	z2	z3	z4	z5	z6	z7	z8	z9	...	z19990	z19991
0	47.453710	738.315292	1976.976484	37.377212	30.890258	328.140130	219.664054	353.867093	54.916013	76.280024	...	43.684104	76.280024
1	82.035032	95.685662	99.631051	40.346459	452.200670	598.035386	42.526961	85.159898	42.526961	1976.976484	...	54.916013	24.907763
2	68.719952	64.287599	113.050168	46.144706	174.736417	37.377212	248.922117	542.435725	60.270636	738.315292	...	85.159898	32.343720
3	1220.480380	452.200670	738.315292	50.244519	28.262542	38.329459	1661.209407	24.407117	85.159898	142.304673	...	35.576168	118.130447
4	149.508847	68.719952	305.120095	56.618735	28.887110	29.532612	108.290699	157.274263	43.684104	62.230529	...	79.079059	64.287599
5	195.276861	2392.141546	54.916013	66.448376	41.415193	39.318566	26.505723	44.889126	108.290699	79.079059	...	25.956397	738.315292

6 rows \times 20000 columns

Figure 4.4: SNR values Data Frame

The proposed DNN approach is implemented in Python 3.6.6 with TensorFlow 2.0.0, one computer node with 3 cores 1.6GHz and 8GB RAM. We set the numbers of hidden layers to 3. The input and the output are set to 300 neurons, the first hidden layers has 200 neurons the second and the third 80 respectively.

4.2.2 Parameters selection and performance of DNN approach

In Figure. 4.5 we present the mean square error (MSE) given by different learning rate. We took the number of $STAs$ to be 30.

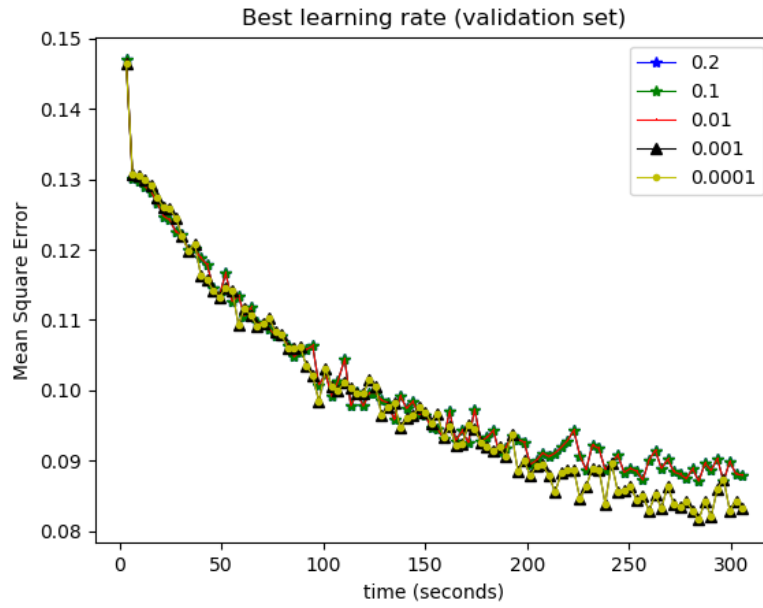


Figure 4.5: learning rate selection

We can see that the lower MSE is given when learning rate is 0.001. To obtain this we used 1000 as batch size, 100 epochs, seed 0 for training set and seed 7 for validation set.

4.2.3 Sum-rate performance

We summarize in table. 4.2 the performance of the DNN approach and the classic BM-IC. We took in account the sum-rate, the computational time and the ratio for different configuration of the network with 10, 20 and 30 *STAs*.

Number of STA	Sum-rate		Ratio DNN/BM-IC	Computational time	
	DNN	BM-IC		DNN	BM-IC
10	2.624	2.792	93.997%	0.048	2.342
20	3.368	3.655	92.136%	0.032	6.926
30	3.549	4.124	86.053%	0.043	13.398

Table 4.2: Sum-rate and computational time performance of DNN and BM-IC

The table show that the sum-rate of both DNN approach and the classic BM-IC increase when the number of *STAs* in the network increase. The ratio decrease when the number of *STAs* increase in the network, this can be explain by the fact that, the more the network is dense the more the interference increase. The computational time of DNN approach is more less than the one of classical BM-IC and it became more important when network is dense as shown in fig. 4.6 below where we had the evolution of sum-rate fig. 4.6a and computational time fig. 4.6b depending of number of *STAs*.

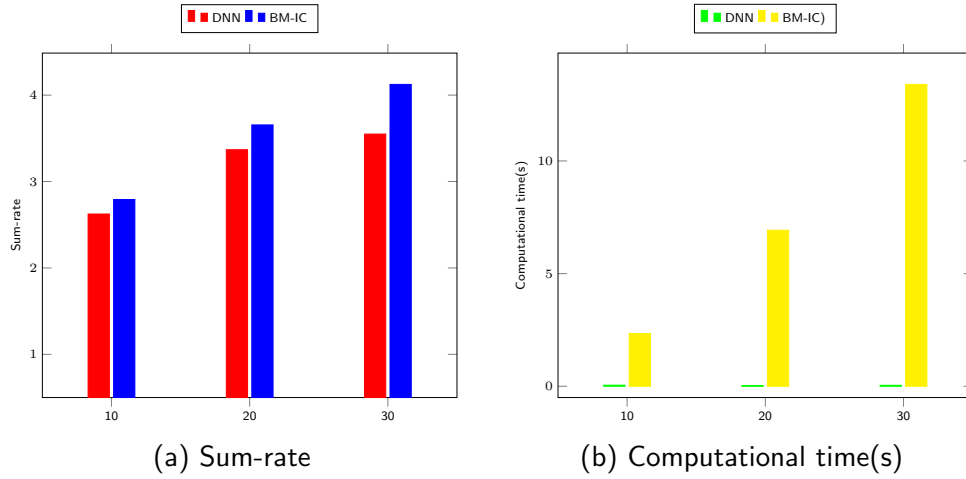


Figure 4.6: Sum-rate and computational time performance of DNN and BM-IC when the number of STA increase

Conclusion

In this chapter we firstly present the impact the number of AP and STA in overhead BFT mechanism and generated the training and testing data set for DNN. We present performance of DNN approach to solve BM-IC problem in dense mm-wave. and it became clearly that DNN approach is more better in point of view of computational time in dense mm-Wave network than classical BM-IC method.

Conclusion and perspectives

A fully operative and efficient 5G network cannot be complete without the inclusion of artificial intelligence (AI). AI and its subcategories like machine learning and deep learning are the relevant techniques that help to improve significantly the mobile network today especially the 5G mobile network. AI and in particular Deep Learning have been introduced these last years in the area of wireless communication to solve complex problem like resources allocations.

The purpose of this thesis was to use Deep Learning in wireless communication to solve the optimization problem, especially to optimize the beamforming in dense mm-Wave networks. For that, we focused on the topic, Deep Learning based 5G mm-Wave beamforming management scheme, where we proceed in several steps. We first built a dense mm-Wave with centralized architecture that contains several *APs* and *STAs* and one master *MAP* in a static configuration, we then perform BFT mechanism between *MAP*, *AP* and *STA* for selected the suitable beam for which each *STAs* will connect to. Secondly we formulated the mathematical problem which was the NP-hard optimization problem and then the proposed approach solution in **algorithm 1** was based on block coordinate descent method where consisted to solve iteratively the problem by fixing some set of parameters and optimized one at the time, that help us to generate the $SNR_{i,j}$ values and different data set for training and testing in Deep learning part. Thirdly, for the deep learning part we constructed a DNN model with multiple hidden layers that work as a linear sub-assignment problem in which each sub-problem received the generated data coming from one optimization problem. The last part devoted to the simulations, shows for BFT mechanism the significant diminution of the overhead compared to the overhead of IEEE802.11ad/ay. The performance evaluation shows that when the number of *STA* increase in the network, the sum-rate of both classic and DNN model also increase while the ratio decrease cause by the augmentation of the interference in the network. We also saw that the computational time in DNN approach is more less than when we used the classic BM-IC method. Based on those results, we can say that DNN approach is the best approach to use in context of dense mm-Wave network.

As perspective of this thesis, we will also conduct a comparative study of our proposed beam selection and other deep learning-based methods as convolutional neural networks and reinforcements learning and we will proceed the same for the dynamical architecture.

References

- Quang Trung Dong, Nuttapol Prayongpun, and Kosai Raoof. Antenna selection for mimo systems in correlated channels with diversity technique. In *2008 4th International Conference on Wireless Communications, Networking and Mobile Computing*, pages 1–4. IEEE, 2008.
- Qing Xue, Xuming Fang, Ming Xiao, Shahid Mumtaz, and Jonathan Rodriguez. Beam management for millimeter-wave beamspace mu-mimo systems. *IEEE Transactions on Communications*, 67(1):205–217, 2018.
- Faizan Qamar, MHD Nour Hindia, Kaharudin Dimiyati, Kamarul Ariffin Noordin, and Iraj Sadegh Amiri. Interference management issues for the future 5g network: a review. *Telecommunication Systems*, 71(4):627–643, 2019.
- Chaoyun Zhang, Paul Patras, and Hamed Haddadi. Deep learning in mobile and wireless networking: A survey. *IEEE Communications Surveys & Tutorials*, 21(3):2224–2287, 2019.
- Tianqi Wang, Chao-Kai Wen, Hanqing Wang, Feifei Gao, Tao Jiang, and Shi Jin. Deep learning for wireless physical layer: Opportunities and challenges. *China Communications*, 14(11):92–111, 2017.
- Pei Zhou, Xuming Fang, Xianbin Wang, Yan Long, Rong He, and Xiao Han. Deep learning-based beam management and interference coordination in dense mmwave networks. *IEEE Transactions on Vehicular Technology*, 68(1):592–603, 2018.
- Shree Krishna Sharma, Tadilo Endeshaw Bogale, Long Bao Le, Symeon Chatzinotas, Xianbin Wang, and Björn Ottersten. Dynamic spectrum sharing in 5g wireless networks with full-duplex technology: Recent advances and research challenges. *IEEE Communications Surveys & Tutorials*, 20(1):674–707, 2017.
- Ado Adamou Abba Ari, Abdelhak Gueroui, Chafiq Titouna, Ousmane Thiare, and Zibouda Aliouat. Resource allocation scheme for 5G C-RAN: a swarm intelligence based approach. *Computer Networks*, 165:106957, 2019.
- Peng Liu, Jiri Blumenstein, Nemanja Stefan Perović, Marco Di Renzo, and Andreas Springer. Performance of generalized spatial modulation mimo over measured 60ghz indoor channels. *IEEE Transactions on Communications*, 66(1):133–148, 2017.
- Ming Xiao, Shahid Mumtaz, Yongming Huang, Linglong Dai, Yonghui Li, Michail Matthaiou, George K Karagiannidis, Emil Björnson, Kai Yang, I Chih-Lin, et al. Millimeter wave communications for future mobile networks. *IEEE Journal on Selected Areas in Communications*, 35(9):1909–1935, 2017.
- Sumit Singh, Raghuraman Mudumbai, and Upamanyu Madhow. Interference analysis for highly directional 60-ghz mesh networks: The case for rethinking medium access control. *IEEE/ACM Transactions on networking*, 19(5):1513–1527, 2011.

- Xiwen Jiang and Florian Kaltenberger. Channel reciprocity calibration in tdd hybrid beamforming massive mimo systems. *IEEE Journal of Selected Topics in Signal Processing*, 12(3):422–431, 2018.
- Xiwen Jiang. *Massive MIMO: turning concept into reality by exploiting the channel reciprocity*. PhD thesis, 2017.
- Hien Quoc Ngo, Erik G Larsson, and Thomas L Marzetta. Massive mu-mimo downlink tdd systems with linear precoding and downlink pilots. In *2013 51st Annual Allerton conference on communication, control, and computing (Allerton)*, pages 293–298. IEEE, 2013.
- ma-mimo.ellintech. Six differences between mu-mimo and massive mimo. Webots, <https://ma-mimo.ellintech.se/2017/10/17/six-differences-between-mu-mimo-and-massive-mimo/>, Accessed April 2020.
- Erik G Larsson, Ove Edfors, Fredrik Tufvesson, and Thomas L Marzetta. Massive mimo for next generation wireless systems. *IEEE communications magazine*, 52(2):186–195, 2014.
- Antoine Roze. *Massive MIMO, une approche angulaire pour les futurs systemes multi-utilisateurs aux longueurs d'onde millimetriques*. PhD thesis, 2016.
- Kinda Khawam, Samer Lahoud, Marc Ibrahim, Mohamad Yassin, Steven Martin, Melhem El Helou, and Farah Moety. Radio access technology selection in heterogeneous networks. *Physical Communication*, 18:125–139, 2016.
- Jiao Wang, Jay Weitzen, Oguz Bayat, Volkan Sevindik, and Mingzhe Li. Interference coordination for millimeter wave communications in 5g networks for performance optimization. *EURASIP Journal on Wireless Communications and Networking*, 2019(1):46, 2019.
- Jingon Joung. Machine learning-based antenna selection in wireless communications. *IEEE Communications Letters*, 20(11):2241–2244, 2016.
- Asside Christian Djedouboum, Abba Ari, Ado Adamou, Abdelhak Mourad Gueroui, Alidou Mohamadou, and Zibouda Aliouat. Big data collection in large-scale wireless sensor networks. *Sensors*, 18(12):4474, 2018.
- Junfei Qiu, Qihui Wu, Guoru Ding, Yuhua Xu, and Shuo Feng. A survey of machine learning for big data processing. *EURASIP Journal on Advances in Signal Processing*, 2016(1):67, 2016.
- Mohammad Abu Alsheikh, Shaowei Lin, Dusit Niyato, and Hwee-Pink Tan. Machine learning in wireless sensor networks: Algorithms, strategies, and applications. *IEEE Communications Surveys & Tutorials*, 16(4):1996–2018, 2014.
- Ahmet M Elbir and Kumar Vijay Mishra. Joint antenna selection and hybrid beamformer design using unquantized and quantized deep learning networks. *IEEE Transactions on Wireless Communications*, 2019.
- Ahmed Alkhateeb, Sam Alex, Paul Varkey, Ying Li, Qi Qu, and Djordje Tujkovic. Deep learning coordinated beamforming for highly-mobile millimeter wave systems. *IEEE Access*, 6:37328–37348, 2018.

- Min Soo Sim, Yeon-Geun Lim, Sang Hyun Park, Linglong Dai, and Chan-Byoung Chae. Deep learning-based mmwave beam selection for 5g nr/6g with sub-6 ghz channel information: Algorithms and prototype validation. *IEEE Access*, 8:51634–51646, 2020.
- Yaping Cui, Xuming Fang, Yuguang Fang, and Ming Xiao. Optimal nonuniform steady mmwave beamforming for high-speed railway. *IEEE Transactions on Vehicular Technology*, 67(5):4350–4358, 2018.
- D Bertsekas and J Tsitsiklis. Parallel and distributed computation: Numerical methods. athena scientific, 1997. *Google Scholar Google Scholar Digital Library Digital Library*.
- Mengyuan Lee, Yuanhao Xiong, Guanding Yu, and Geoffrey Ye Li. Deep neural networks for linear sum assignment problems. *IEEE Wireless Communications Letters*, 7(6):962–965, 2018.
- Chafika Benzaid and Tarik Taleb. Ai-driven zero touch network and service management in 5g and beyond: Challenges and research directions. *IEEE Network*, 34(2):186–194, 2020.